https://doi.org/10.5194/egusphere-2026-2030
Preprint. Discussion started: 22 April 2026


# Ion composition of the Earth plasmasphere observed by the PEP JEI and RPWI instruments on the JUICE spacecraft

Markus Fränz[1], Henning Fischer[1], Norbert Krupp[1], Elias Roussos[1], Philipp Wittmann[1], Patrick Bambach[2], Jan-Erik Wahlund[3], Gabriella Stenberg Wieser[4], Stas Barabash[4], Mika Holmberg[5], Maryam Zeroual[5], Pontus C. Brandt[6], Peter Wurz[7], Martin Wieser[4], Yoshifumi Futaana[4], Manabu Shimoyama[4], Angèle Pontoni[4], Audrey Vorburger[7], André Galli[7], Andreas Riedo[7], George Ho[6], Donald G. Mitchell[6], George Clark[6], Peter Kollmann[6], Malamati Gkioulidou[6], Leonardo Regoli[6], Robert Wimmer-Schweingruber[8], Kazushi Asamura[9], Esa Kallio[10], Andrea Opitz[11], Manuel Grande[12], Andrew Coates[13], Geraint Jones[13], Theodoros Sarris[14], Andrey Fedorov[15], Nicolas André[15,17], and Ján Baláž[16]

[1]Max-Planck-Institut für Sonnensystemforschung, Göttingen, Germany
[2]Deutsches Zentrum für Luft- und Raumfahrt, Cologne, Germany
[3]Swedish Institute of Space Physics (IRF),Uppsala, Sweden
[4]Swedish Institute of Space Physics (IRF),Kiruna, Sweden
[5]Astronomy Astrophysics Section, School of Cosmic Physics, Dublin Institute for Advanced Studies, DIAS Dunsink Observatory, Dublin, Ireland
[6]Johns Hopkins University, Baltimore, MD, USA
[7]Space Research & Planetary Sciences, University of Bern, Switzerland
[8]Christian-Albrechts-Universität zu Kiel, Kiel, Germany
[9]Institute of Space and Astronautical Science, Sagamihara, Japan
[10]Department of Electronics and Nanoengineering, School of Electrical Engineering, Aalto University, Espoo, Finland
[11]Institute for Particle and Nuclear Physics, Wigner Research Centre for Physics, Budapest, Hungary
[12]Institute of Mathematical and Physical Sciences, University of Wales Aberystwyth, Wales, United Kingdom
[13]Mullard Space Science Laboratory, University College, London, United Kingdom
[14]Department of Electrical and Computer Engineering, Democritus University of Thrace, Xanthi, Greece
[15]Institut de Recherche en Astrophysique et Planétologie (IRAP), CNES-CNRS-Université Toulouse III Paul Sabatier, Toulouse, France
[16]Institute of Experimental Physics SAS, Košice, Slovak Republic
[17]Institut Supérieur de l'Aéronautique et de l'Espace (ISAE-SUPAERO), Université de Toulouse, Toulouse, France

**Correspondence:** Markus Fränz (fraenz@mps.mpg.de)

**Abstract.** During the first Earth gravity assist maneuver of JUICE on 20th August 2024 the spacecraft passed through the Earth plasmasphere for about 2 hours. Before closest approach at a distance of 2.1 $R_E$ the Jovian Electron and Ion spectrometer JEI of the PEP instrument suite was switched on for 40min in an ion mode test configuration. The high plasma density of about 3000/$\mathrm{cm}^3$ (observed by the RPWI plasma wave instrument) led to a negative charging of the spacecraft which allowed a rare observation of the cold and dense plasmaspheric ion populations. Since the ions are only corotating with the Earth at a velocity of about $1\mathrm{km/s}$ at this distance the observed ion speed is dominated by the spacecraft velocity of about $8\mathrm{km/s}$. For this reason ions with different mass appear at different energies in the energy spectrum observed by the JEI sensor. In addition the spacecraft potential leads to specific filtering of ion masses in the observed angular distribution. By calculating the sensor

https://doi.org/10.5194/egusphere-2026-2030
Preprint. Discussion started: 22 April 2026


response function for these specific observing conditions it is possible to quantify densities of the different ion species. But this response calculation depends critically on the response of the JEI channel electron multipliers to the ion velocity and mass. Since the sensor was operated with a low post-acceleration further laboratory calibrations may be needed for this specific setup. Still we can already conclude from the observations that ions with mass $> 4\mathrm{amu/q}$ contribute at least 30% to the observed total ion density. A flux peak observed in the energy spectrum at $15\mathrm{eV}$ can only be explained by the presence of heavy molecular ions with mass $\sim 30\mathrm{amu/q}$. Molecular ions have only been rarely detected in the outer Earth plasmasphere. The observations indicate that the JEI sensor can also be used to achieve ion composition measurements in the exospheres of the Jovian moons.

## 1 Introduction

On the 20th August 2024 the JUICE spacecraft (Grasset et al., 2013) made its first gravity assist maneuver at Earth with a closest approach altitude of 6850 $\mathrm{km}$ corresponding to a L-shell of $2.31 R_E$. At this distance from Earth the spacecraft encountered the Earth plasmasphere and several sensors - originally designed for measurements at Jupiter - were able to make new observations of the Earth plasmasphere. Here we report on the measurements of the Jovian Ion and Electron spectrometer (JEI) which is one of the thermal plasma sensors of the Particle Environment Package (PEP, Barabash (2026)) onboard JUICE. The observations are supported by measurements made by the Radio & Plasma Wave Investigation (RPWI, Wahlund et al. (2025)).

### The Earth plasmasphere

The Earth plasmasphere is a region of dense cold plasma extending between 1.5 and about 6 Earth radii ($R_E$) around Earth (Darrouzet et al., 2009). The plasmaspheric ion density is usually $> 10^3/\mathrm{cm}^3$ within $3R_E$ with a plasma temperature $< 1$ $\mathrm{eV}$. Because the plasmaspheric ion population is rotating close to corotation with Earth, it has very low energy ($< 10$ $\mathrm{eV}$) in the frame of typical spacecraft observations. This means the ion properties can only be measured in-situ with retarding potential analyzer (RPA) techniques or when the spacecraft charges negatively. The first detailed analysis of the effect of the spacecraft potential on the plasmaspheric spectrum was provided by Whipple et al. (1974) using data obtained by the RPA instrument on the OGO-3 satellite. The most relevant cold ion composition measurements available until today were made by the RPA instrument RIMS onboard Dynamics Explorer 1 (DE 1) between 1981 and 1984 (Roberts et al., 1987). This instrument could in principle measure ions up to mass 32 (Chappell et al., 1981) the continuously downlinked dataset contains only observations of $H^+$, $He^+$, $He^{++}$, $O^+$ and $O^{++}$ (Roberts et al., 1987). This dataset was reviewed by Goldstein et al. (2018) where it is stressed that specifically the oxygen density of the outer plasmasphere ($> 2R_E$) is highly variable and can reach beyond $1000/\mathrm{cm}^3$ such that a specific oxygen torus might form. But on a single specific orbit during a magnetic storm the RIMS instrument was operated in a mode which allowed observation of heavier ions up to mass 46 (Craven et al., 1985). On this orbit a strong flux of ions with 28, 20 and 32 $\mathrm{amu/q}$ with similar relative abundance was observed stretching from L=1.1$R_E$ to $3R_E$. These were interpreted as $N_2^+$, $NO^+$ and $O_2^+$ ions. Interestingly the flux at larger distances was observed to be accelerated along the magnetic field. These observations agreed with earlier observations by the ion mass spectrometer

https://doi.org/10.5194/egusphere-2026-2030
Preprint. Discussion started: 22 April 2026


on the ISIS-2 spacecraft during a magnetic storm at 1400km altitude (Hoffman et al., 1974). The accelerated thermal plasma was even sometimes observed at the Earth magnetopause (Sauvaud et al., 2001). Recently Yue et al. (2023) also reported on observations of plasmaspheric cold ions by the the Van-Allen-Probe HOPE instrument. All observations of molecular ion outflow from the ionosphere up to 2022 were reviewed by Lin and Ilie (2022) and Yamauchi et al. (2024). From these reviews it becomes clear that all more recent observations are for energized outflow (with energies >100eV) while the cold plasmaspheric composition has not been observed again after the DE-1 measurements in 1984. A problem with the DE-1 measurements was that the spacecraft potential was not observed by an independent instrument during the observations (Comfort et al., 1985). Ion temperature and potential were obtained by an iterative fit to the data resulting in a plasmaspheric temperature of about 3000–5000K(0.27–0.45eV) at $L = 2R_E$ (Comfort, 1996). But the authors emphasize that without knowledge of the potential the ion temperature may be overestimated. The importance of the cold ion population for magnetospheric dynamics was discussed by Delzanno et al. (2021). A comprehensive review of the instrumental limitations of cold ion observations can be found in Maldonado et al. (2023).

The rather high plasmaspheric temperatures (>0.5 eV) compared to ionospheric temperatures (<0.1 eV) observed by these early RPA instruments did pose a problem for plasma theory because no sufficient heating mechanism could be identified (Gringauz, 1983). Proton temperatures were again determined from 1996-2001 by the RPA instrument on the MAGION-5 sub-satellite of the INTERBALL 2 mission. Analysis of this data set by Kotova et al. (2008) showed that the temperature of the inner plasmasphere is closely correlated to the temperature of the upper ionosphere. Local temperature is anti-correlated to local density and drops to values below 2000 K(0.18 eV) for densities > 2000/$\mathrm{cm}^3$ confirming that the earlier RPA analyses may have overestimated the temperatures. The plasmaspheric temperature observations were discussed again in context of the Van-Allen-Probe mission Genestreti et al. (2017) where proton temperatures were determined by indirect methods for two orbits confirming the results of Kotova et al. (2008). We note that the Van-Allen-Probe spacecraft charged positive in the plasmasphere which inhibited the direct observation of cold ions (Jahn et al., 2020).

## 2 The observation by the JUICE spacecraft

The ESA spacecraft JUICE was launched on 14th April 2023 on its long mission to planet Jupiter. Between the 19th and 21st August 2024 the spacecraft conducted the first ever Lunar - Earth gravity assists (LEGA) maneuver. The trajectory of the spacecraft during the Lunar - Earth flyby is shown in Figure 1 projected onto the geocentric solar ecliptic (GSE) XY-plane. Overplotted are the orbit of the Moon (red crosses), the expected position of the Earth plasmapause (red dots), magnetopause (green) and bowshock (cyan). The JEI sensor of the PEP instrument suite (Barabash, 2026) was switched on only during 4 time intervals of length 40min. These 4 intervals are indicated by the coloring along the JUICE trajectory which shows the count rate observed by channel 15 of the JEI sensor, which shows the highest count rates. The intervals were chosen to obtain electron measurements around the Moon and magnetopause and ion measurements in the plasmasphere and around the bow shock. In this paper we only discuss the observations made during the plasmasphere crossing. An enlarged plot of this crossing is shown in Figure 2 in the same coordinate plane as Figure 1. The JEI sensor obtained science data on 20th August 2024

https://doi.org/10.5194/egusphere-2026-2030
Preprint. Discussion started: 22 April 2026


from 21:19 to 21:56 UTC just before closest approach to the Earth at 21:56:14 UTC. At this point the JUICE spacecraft had a distance of 13211 km or altitude of about 6850 km at geographic latitude 24.0$^o$ and L-shell 2.31 $R_E$.

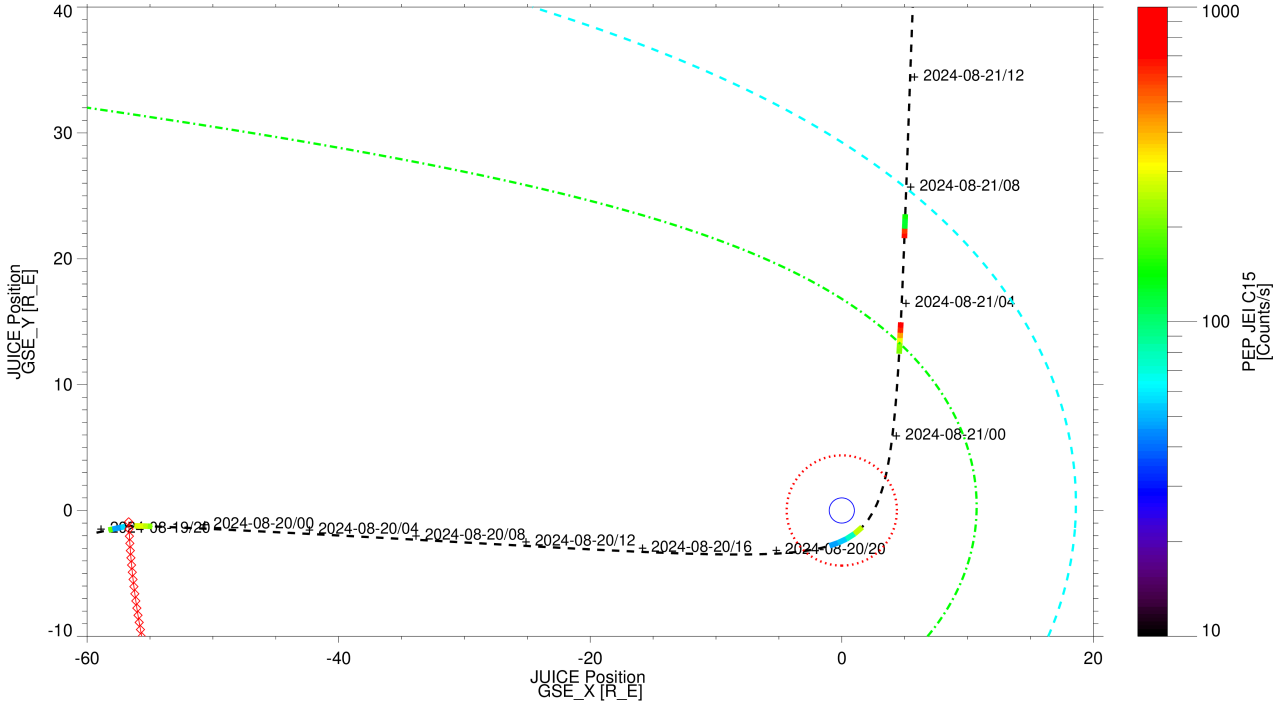


**Figure 1.** Trajectory of JUICE (black line) during the flyby of the Moon (lower left corner, red crosses) and the Earth on 21st August 2024 in the GSE XY plane. The different lines show nominal position of the plasmapause (red, dotted) (Larsen et al., 2007), the magnetopause (green, dash dot) (Shue et al., 1998) and bow shock (cyan, dashed) (Lu et al., 2019). The colored sections along the JUICE trajectory show the operation times of PEP JEI where the color indicates the count rate observed in channel 15.

Figure 3 shows the densities of $H^+$, $He^+$ and $O^+$ predicted for the position of JUICE by the Earth global core plasmasphere model (Gallagher et al., 2000) for a Kp value of 1.7 which was prevalent during the JUICE closest approach (https://kp.gfz.de/en/). The model predicts a sharp inbound plasmapause. The authors of the model note that specifically the $O^+$ density is highly variable and the model assumes constant initial ratios of 0.1 for $He^+$ and 0.01 for $O^+$ relative to $H^+$. Molecular ions are not contained in the model. We may just consider the total peak ion density value of about 4000/cm$^3$ predicted by the model and note that the SPICED model for the equatorial plasmasphere predicts for L=2 $R_E$ and MLT = 6h an average density of 2200/cm$^3$ (James et al. (2021), their Fig. 12).

### 2.1 Observation geometry

Figure 4 shows the orientation of the JUICE spacecraft relative to Sun (yellow) and Earth together with the orientation of the geocentric solar magnetic (GSM) axes and the spacecraft velocity vector (cyan) at 20th August 2024 21:30UTC. The yellow

https://doi.org/10.5194/egusphere-2026-2030
Preprint. Discussion started: 22 April 2026


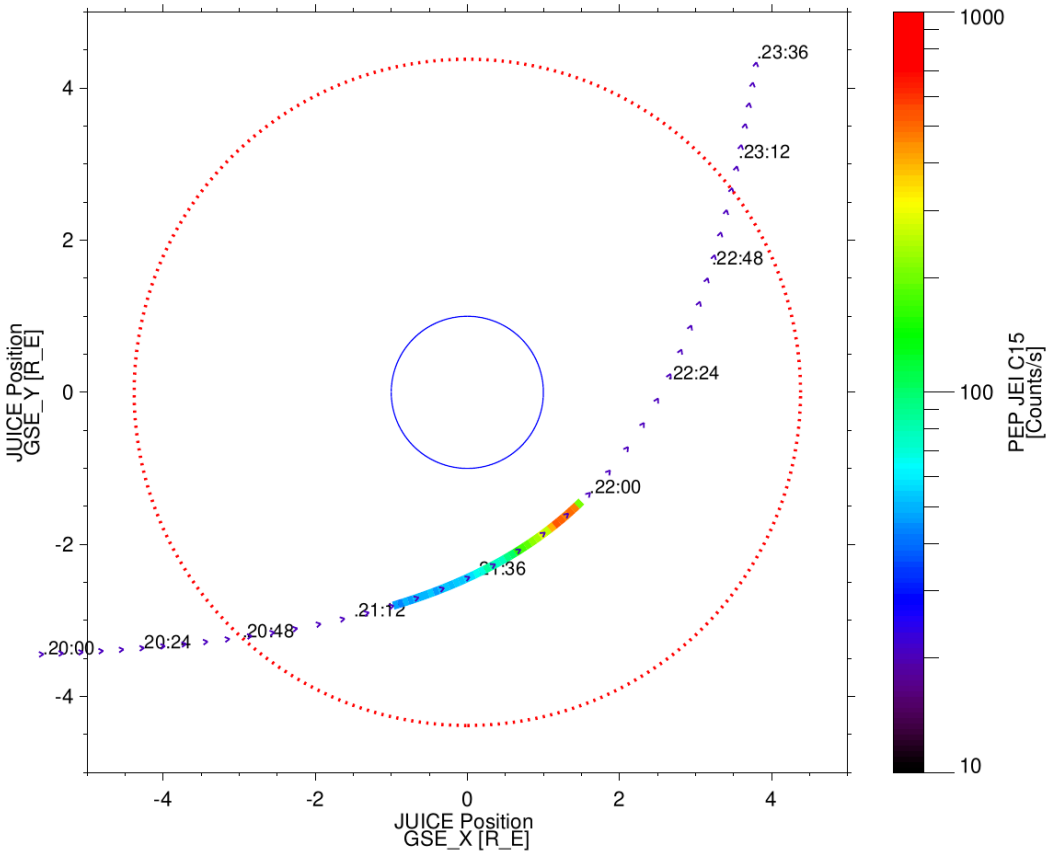


**Figure 2.** Trajectory of JUICE (blue symbols) during the flyby of the Earth on 21st August 2024 in the GSE XY plane. The red dotted line shows the nominal position of the plasmapause (Larsen et al., 2007). The colored section along the JUICE trajectory shows the operation time of PEP JEI where the color indicates the count rate observed in channel 15. Blue arrows indicate the JUICE velocity vector direction.

line indicates the Earth terminator. This principal orientation of the spacecraft was maintained throughout the observation interval. The PEP JEI sensor is mounted on the spacecraft panel which looks towards Earth during this time. This panel is illustrated in Figure 5 which shows the location of the NIM, JNA and JEI sensors together with the orientation of the body fixed spacecraft coordinate system axes, the direction of Earth and Sun and the spacecraft velocity vector relative to Earth. The body fixed spacecraft Z-axis coincides with the JEI sensor symmetry axis. The JEI polar field of view extends from $8^o$ to $78^o$ from this axis. In Figure 5(right) we also show the field of view of JEI azimuth sectors 1, 0, 15 and 14.

Figure 6 shows position and velocity parameters of the JUICE spacecraft relative to Earth for the period of the plasmasphere crossing, from top to bottom: spacecraft position in GSM coordinates in Earth radii ($R_E$), spacecraft GSM and GSE latitude, magnetic field **Bgeo** (nT) in spacecraft coordinates predicted by the Tsyganenko96 model (Tsyganenko and Stern, 1996), spacecraft velocity vector (km/s), and the plasma corotation velocity vector (km/s), the difference vector **D** between both in

https://doi.org/10.5194/egusphere-2026-2030
Preprint. Discussion started: 22 April 2026


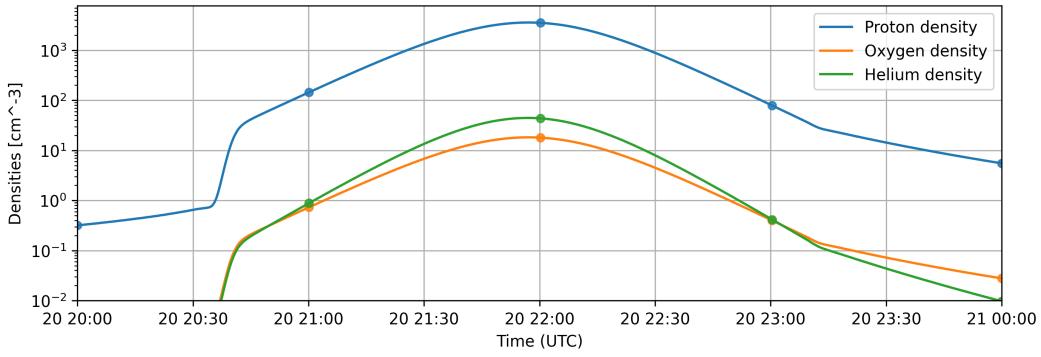


**Figure 3.** $H^+$, $He^+$ and $O^+$ densities predicted for the trajectory on the 20 August 2024 of JUICE by the Earth global core plasmasphere model (GCPM v2.4, Gallagher et al. (2000)).

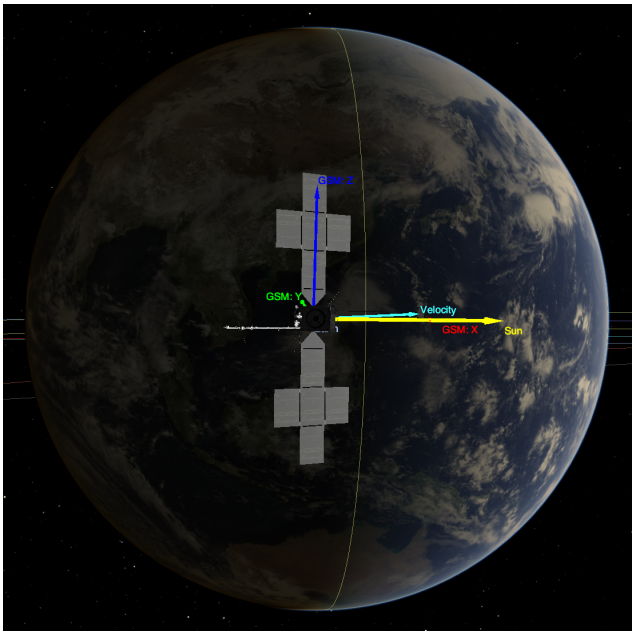


**Figure 4.** View of Earth from JUICE at 20th August 2024 21:30 UTC with the GSM frame axes. The Earth terminator (yellow) is almost parallel to the GSM Z-axis. The spacecraft velocity vector relative to Earth (cyan) is in the GSM XY-plane. Figure produced by the JUICE Cosmographia software (https://www.cosmos.esa.int/web/spice/cosmographia).

JUICE spacecraft coordinates, and the angles of **D** and **Bgeo** in spacecraft coordinates. We here assume that the corotation is symmetric around the GSM Z-axis. Models of the corotation predict ∼92% corotation at L=2.0 (Lejosne et al., 2017). Vector components are indicated by X(blue), Y(green), Z(red) and total T(black). The red vertical line indicates the closest approach (CA) and the blue frame the period of the JEI observation discussed in the following. Calibrated onboard magnetic field data

https://doi.org/10.5194/egusphere-2026-2030
Preprint. Discussion started: 22 April 2026


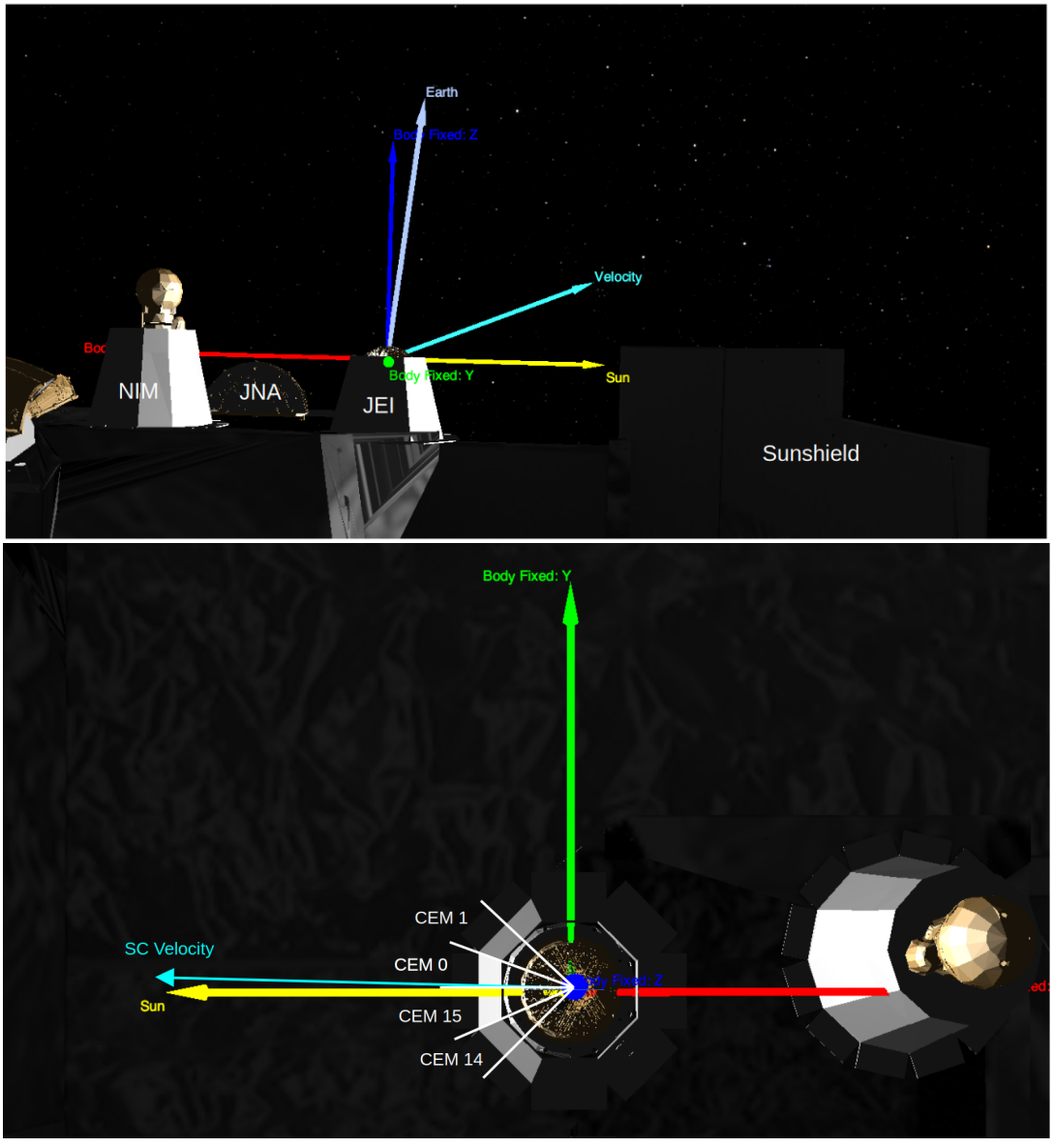


**Figure 5.** View of PEP sensors on the nadir deck of the JUICE spacecraft. The JUICE JEI coordinate frame orientation (Z=blue, X=red, Y=green) and spacecraft velocity vector relative to Earth (cyan) at 20th August 2024 21:30 UTC are centered at the JEI ion optics entrance. Top: View of the spacecraft frame XZ plane. Bottom: View of the spacecraft frame XY plane, including the field of views of the JEI CEMs. Figure produced by the JUICE Cosmographia software.

are not available at the time of writing. We observe that the predicted magnetic field vector and the spacecraft velocity vector are both at a polar angle of $50^0$ as seen from the JEI sensor.

https://doi.org/10.5194/egusphere-2026-2030
Preprint. Discussion started: 22 April 2026


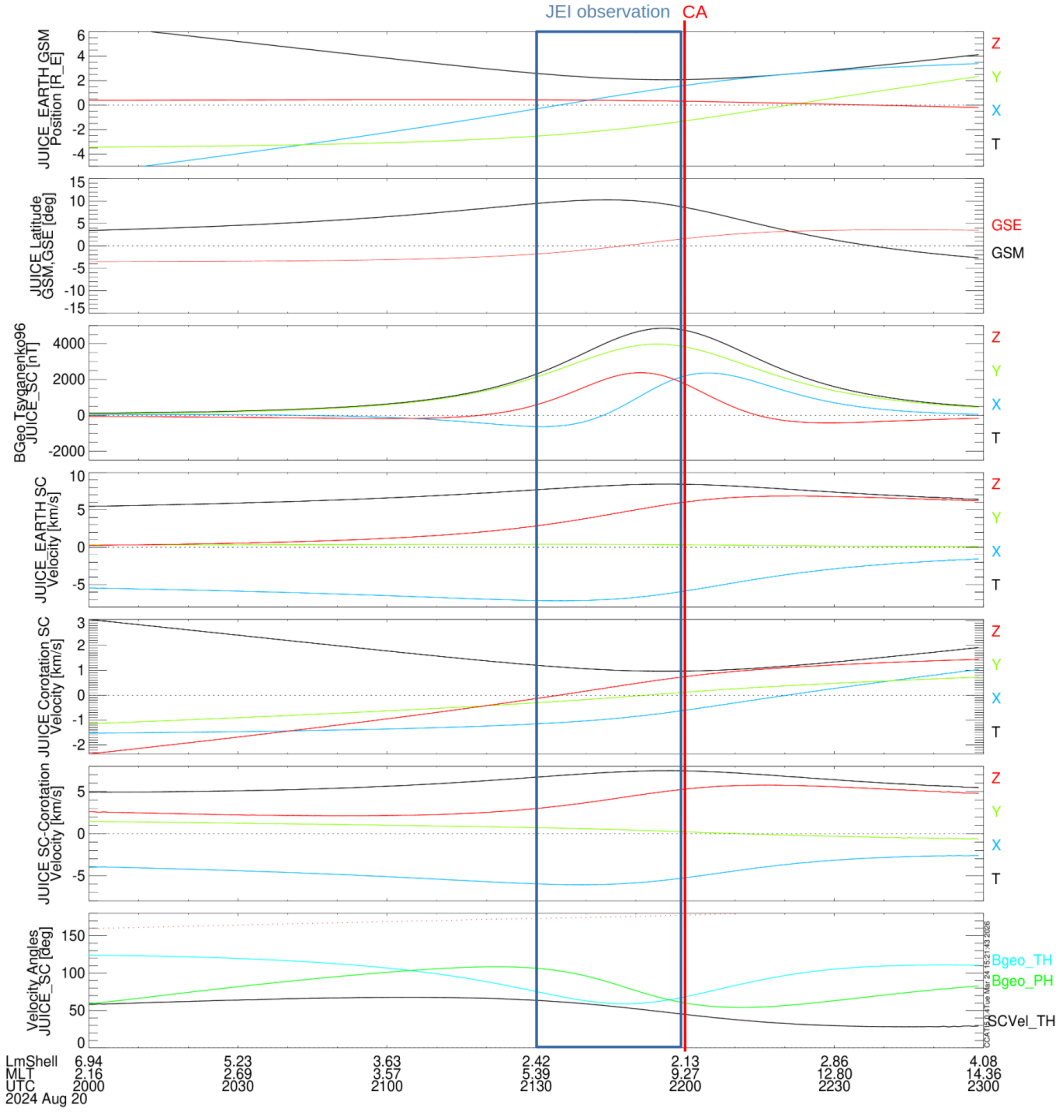


**Figure 6.** JUICE orbital parameters in Earth centered coordinates for 20:00-23:00 UTC on 20th August 2024 from top to bottom: Position vector components in GSM coordinates, GSM (black) and GSE (red) latitude, Tsyganenko96 geomagnetic field **Bgeo** at JUICE position in spacecraft coordinates, JUICE velocity vector relative to Earth in spacecraft coordinates, plasma corotation vector at full corotation in spacecraft coordinates, difference vector **D** between JUICE velocity and corotation, $\theta$ angle of **D** (black) and **Bgeo** (cyan) and $\phi$ angle of **Bgeo** (green). The Tsyganenko field and $L_m$-shell values are calculated using the IRBEM model of the disturbed geomagnetic field for the solar wind conditions prevalent during the JUICE passage (https://prbem.github.io/IRBEM/index.html).

https://doi.org/10.5194/egusphere-2026-2030
Preprint. Discussion started: 22 April 2026


## 2.2 Instrumentation

The Jovian Electron and Ion Analyzer (JEI) (Fränz et al., 2017) is one out of six sensors of the Particle Environment Package PEP onboard the Juice spacecraft (Barabash, 2026). It is specifically designed to operate in the harsh Jovian environment. The goals of JEI are to measure the electron and ion distribution functions in the energy range from 1 eV to 60 keV with high sensitivity and time resolution and with a hemispherical field of view. For a full list of sensor properties refer to Table A1. The derivation of the spacecraft potential from the Langmuir probe observations of the RPWI instrument on JUICE are described in Wahlund et al. (2025).

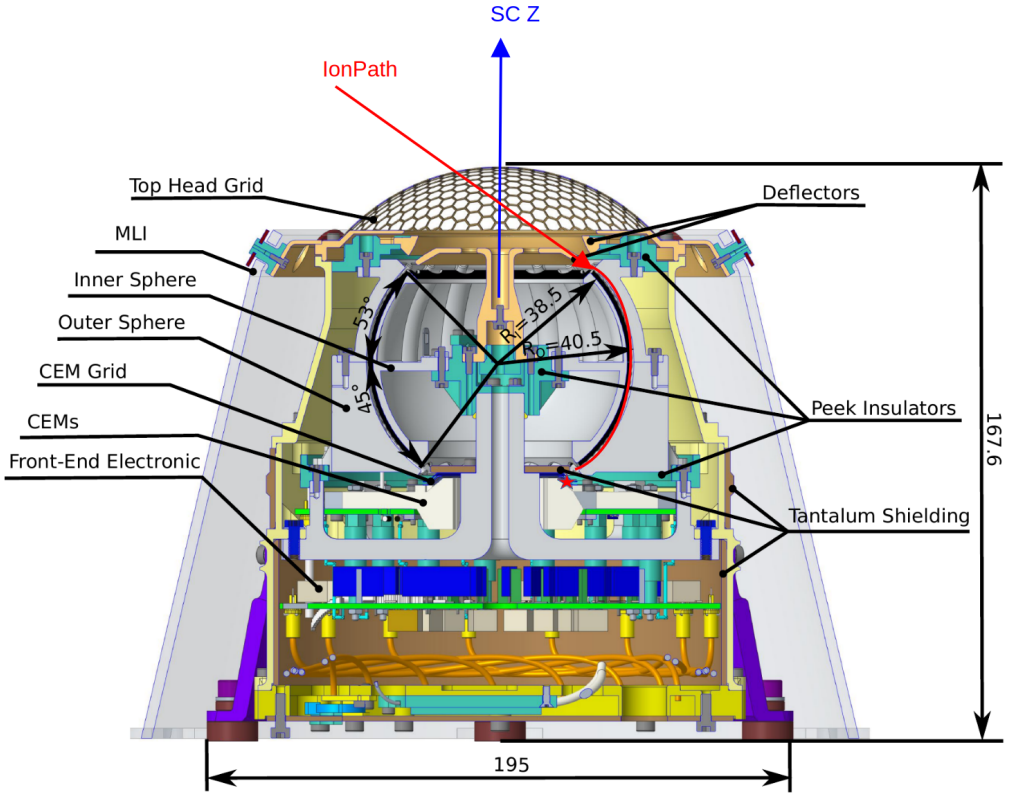


**Figure 7.** Cross-sectional view of the JEI sensor showing the principal components. The sensor is a spherical electrostatic analyzer with an 'open-head' deflection system. Before ions or electrons (red trace) enter the spherical electrostatic analyzer the possible polar entrance angle is set by the deflectors. After the electrostatic analyzer ions are post-accelerated towards the ceramic channel electron multiplier (CEM) entrance, where they create an electric signal (adapted from Bambach (2026)).

Figure 7 shows a cross-sectional view of the JEI sensor with a typical ion path (red). The incoming polar angle with respect to the sensor Z-axis is selected by the deflection system. The ion energy is selected by the spherical analyzer (*Inner and*

https://doi.org/10.5194/egusphere-2026-2030
Preprint. Discussion started: 22 April 2026


*Outer Sphere*). The polarity of the deflectors and analyzer can be switched to allow measurement of both positive and negative particles including electrons. After post-acceleration charged particles are detected by one of 16 ceramic channel electron multipliers (*CEMs*), determining the azimuth angle.

The post-acceleration voltage applied between spherical analyzer and CEM entrance we call *CEM_head* voltage. The detection efficiency is influenced by the CEM_head voltage and the bias-voltage setting across the CEM (*CEM_draw* voltage). The sensor can operate either continuously in electron or ion mode, or it can alternate between both modes about every 8 s. During the plasmasphere observation JEI was operated in ion mode only with a CEM_head voltage of –250V and a CEM_draw voltage of +2100V. At this setting the detection efficiency for protons is about 80%, the detection efficiency for heavier ions is lower as discussed by Krems et al. (2005). Later during the JUICE mission these voltages will be increased to achieve optimum efficiency.

JEI has a minimum time resolution of 4 $\mathrm{ms}$ per energy step , an intrinsic polar resolution of $\sim 5^o$, and energy resolution of $\sim$8% (see Table A1). For a mono-directional beam the energy resolution is around $\sim$5%. Elevation and energy stepping as well as integration time are set by a look-up-table and change with sensor mode. During the plasmasphere observation integration time was set to 4 $\mathrm{ms}$ with a data acquisition time of 3 $\mathrm{ms}$ per energy step, polar stepping was set to 8 polar steps covering a polar range from $14^o$ to $75^o$, and energy stepping was linear in the low energies (0 $\mathrm{eV}$ to 20 $\mathrm{eV}$) with a step width of 0.49 $\mathrm{eV}$ and logarithmic for higher energies up to 10 $\mathrm{keV}$ with a total of 128 energy steps and a duration of 512 $\mathrm{ms}$ for one scan. The average geometric factor of the angular channel 15 of the sensor has been determined in laboratory calibration as $G_E = 3.0 \cdot 10^{-5}$ $\mathrm{cm^2 sr\ eV/eV}$ for an isotropic plasma distribution at pre-acceleration voltage of –1000V with a nitrogen ion beam of 10 $\mathrm{keV}$ energy (Bambach, 2026).

### 2.3 Ion energy spectra and potential

Figure 8 shows the energy spectra obtained by the 4 azimuthal sectors (CEM channels) viewing around the direction azimuth of the spacecraft velocity during the time interval 21:30–21:56 UTC on 20th August 2024. We here show only the spectral energy range 0-20 $\mathrm{eV}$. The higher energy range is dominated by background noise. The white line plotted over the spectra shows the negative value of the spacecraft potential measured by the JUICE RPWI instrument. We observe that all 4 channels observe an intense low energy ion spectrum with a mean energy proportional to the negative spacecraft potential observed by RPWI. The same effect was observed on the opposite side of the spacecraft by the Jovian Plasma Dynamics and Composition analyzer (JDC) of the PEP suite. These observations are discussed in an accompanying paper (Stenberg Wieser et al., 2026). It is interesting to note that the RPA instrument on the OGO-3 spacecraft in 1966 measured at the same L-shell location 1.5–2.5 $R_E$ a very similar potential between –5.0 and –6.0V at an estimated ion density of about 6000/$\mathrm{cm^3}$ (Whipple et al., 1974).

Channel 15 observes the highest flux, though the spacecraft velocity vector is at the edge of the field-of-view of channel 0 (see Figure 5). The reason may lie on the one hand in differences of the detection efficiency of the CEMs at the low CEM_draw voltage setting or in the asymmetric shape of the spacecraft potential. The rather strong signal in the neighboring channels 1 and 14 indicates that the spacecraft potential has a focusing effect, although we can not exclude some electronic and geometric cross talk between the channels as discussed in Bambach (2026). In the following we only discuss the spectra obtained by

https://doi.org/10.5194/egusphere-2026-2030
Preprint. Discussion started: 22 April 2026


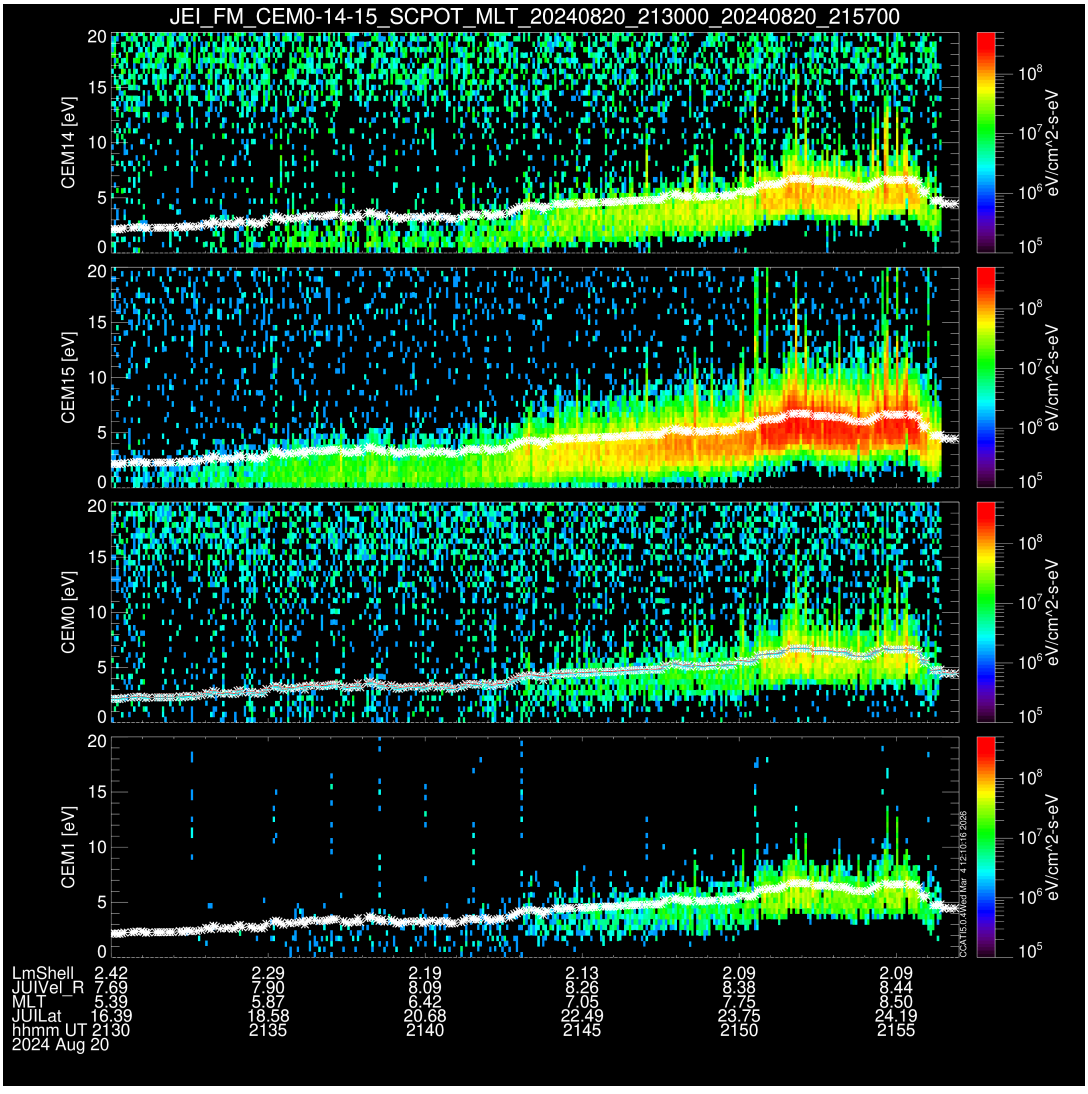


**Figure 8.** Ion energy spectra observed by PEP JEI in 4 azimuthal viewing directions during the passage of the Earth plasmasphere. The median electric background noise has been subtracted from the spectra. White lines show the negative spacecraft potential observed by JUICE RPWI where the left axis gives the negative voltage. Data are averaged over 8 elevation scans (4.6s). Magnetic LShell [$R_E$], local time [h], latitude [deg], total spacecraft velocity, and UTC are noted along the bottom axis.

channel 15 as this has the best counting statistics. While an acceleration by the spacecraft potential should lead to the cold thermal spectrum observed for most energy scans the higher energy spectral peaks observed sporadically caught our attention because they were unexpected.

The top panel of Figure 9 is a zoom into the energy spectra of channel 15 for the one minute time interval between 21:51:30-21:52:20 UTC on 20th August 2024. Overplotted in red is the negative of the spacecraft potential of about –6.5V measured by

https://doi.org/10.5194/egusphere-2026-2030
Preprint. Discussion started: 22 April 2026


RPWI. We observe that the energy spectra show a pattern repeated for each sequence of 8 elevation scans of the sensor. Figure 9 (bottom) shows the mean polar angle of the JEI field-of-view for each spectrum. Overplotted in red is the polar angle of the spacecraft velocity vector relative to Earth. We can see that ions are only observed at polar angles from $14^o$ to about $60^o$. The mean energy of the spectrum is increasing with polar angle. High energy spikes are only observed twice during this interval at 21:51:49 and 21:51:08 UTC at polar angles of about $35^o$.

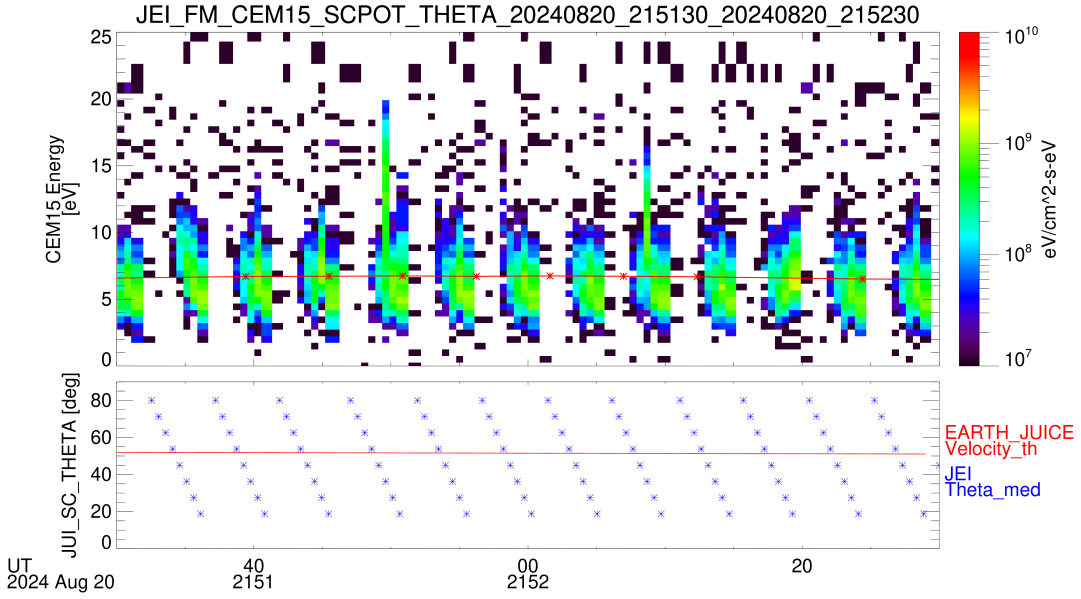


**Figure 9.** Top: Ion energy spectra observed over 1 minute (21:51:30–21:52:30 UTC on 20th August 2024) at 512 ms resolution by PEP JEI CEM15 during the passage of the Earth plasmasphere. The negative of the spacecraft potential value is overplotted in red. Bottom: The median polar angle of each spectra (blue stars) with respect to the Spacecraft Z-axis and the polar angle of the JUICE spacecraft velocity (red line) relative to the Earth.

To further illustrate the effect we show in Figure 10 four individual spectra obtained in sequence around 21:51:49 UTC at different mean polar angles. The top row of the figure shows the counts obtained in each 3 ms energy bin and the value of the mean polar angle ($\theta$). The energy axes show the energy in the JEI reference frame without correction for the spacecraft potential. We note that the statistical error of these spectra can be obtained by the square root of the counts. The bottom row shows the same spectra converted to phase space density assuming an ion mass of 1 amu and a base geometric factor as provided in Table A1 without considering CEM efficiencies. Spectra which show an approximate Maxwellian shape have been fitted with a Maxwellian with the three free parameters mean energy, temperature and density (see Appendix B). The resulting values and their fit standard deviation are printed in addition to the fitted curve (cyan). The plots are in log scale and the fit parameters are derived from 6 data points with the highest phase space density. We can see that the spectra obtained at

https://doi.org/10.5194/egusphere-2026-2030
Preprint. Discussion started: 22 April 2026


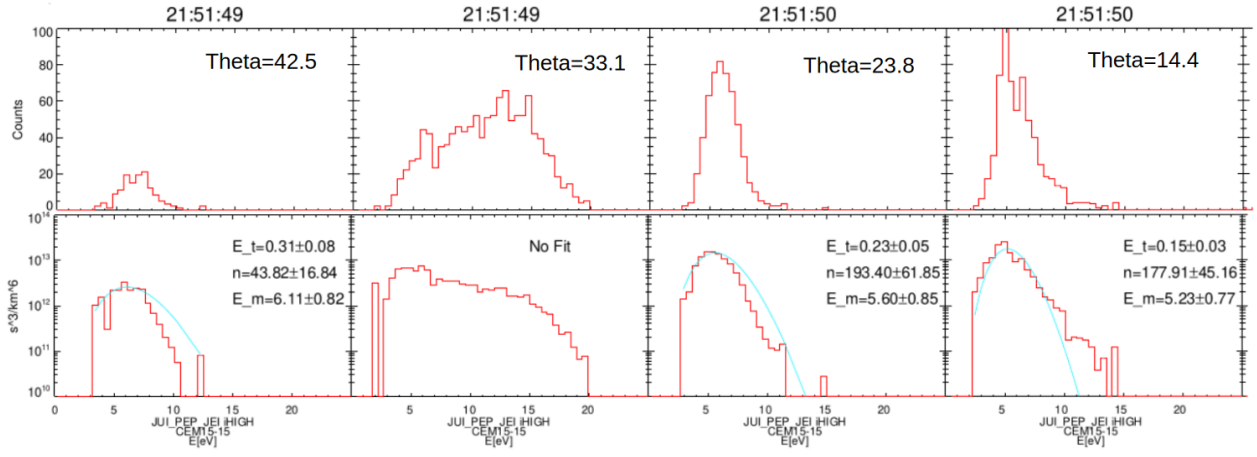


**Figure 10.** Four individual ion spectra observed in sequence around 21:51:49 UTC on 20th August 2024 by PEP JEI CEM15 without correction for the spacecraft potential. Top: Counts in linear scaling. Bottom: Conversion to phase space density assuming proton mass in logarithmic scaling. Some of the spectra allow a Maxwellian fit to the core distribution shown in blue with the derived parameters temperature ($E_t$[eV]), density (n[/cm$^3$]) and mean energy ($E_m$[eV]) in the spacecraft frame of reference.

polar angles $\theta = 14.4^o$ and $\theta = 23.8^o$ can be best approximated by a Maxwellian resulting in ion densities of around 180/cm$^3$, temperatures of around 0.2 eV and mean observed energies around 5.3 eV (including spacecraft potential). As we discuss later the rather low density value as compared to the RPWI value is caused by not considering the geometry and CEM efficiency in this simple approach. When looking closer at the count spectrum obtained at $\theta = 14.4^o$ one can discern 2 peaks in the spectrum which may indicate a bimodal distribution. The most interesting spectrum is the one obtained at $\theta = 33.1^o$. It shows different spectral peaks at higher energies with a statistical significance > $2\sigma$. For this reason we show an enlarged view of this spectrum in Figure 11 where we associate the different peaks with different ion species as explained in the next section.

Before discussing this observation we need to consider the total plasma density and shape of the spacecraft potential. The JUICE RPWI instrument reports an ion density of 3000/cm$^3$ determined by the Langmuir probe measurement for the time 21:55:17 UTC (J.E. Wahlund, personal communication). This agrees approximately with the value of 4000/cm$^3$ predicted by the global plasmasphere model (Figure 3) when taking into account the large temporal variation of the plasmasphere. The electron temperature determined by the RPWI analysis is 0.35–0.5 eV. In this case the plasma Debye length around the spacecraft, which determines the extension of the spacecraft potential, is only about 8.0 cm. This means that the equipotential surfaces follow the shape of the spacecraft structures and must be considered locally as planar and not spherical (see Appendix C). In an accompanying paper Zeroual et al. (2026) discuss the surface charging of the JUICE spacecraft during the Earth gravity assist.

https://doi.org/10.5194/egusphere-2026-2030
Preprint. Discussion started: 22 April 2026


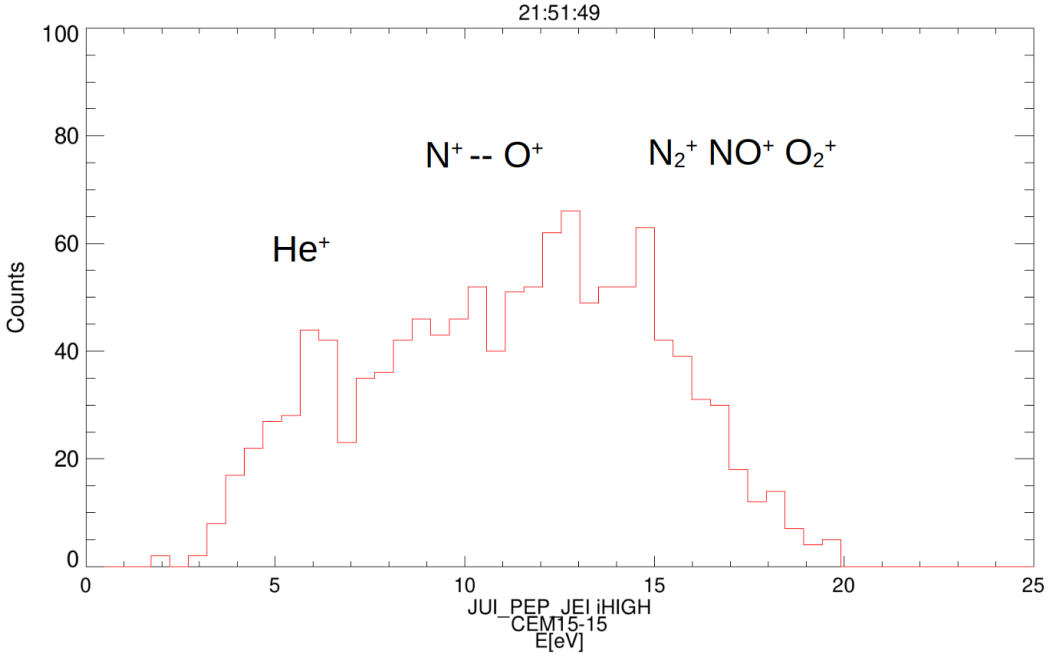


**Figure 11.** Count spectrum observed at 21:51:49 UTC by PEP JEI CEM15 at a polar deflection angle of 33.1$^o$ and attribution of flux peaks to species. The association of the spectral peaks with different ion species is explained in context of Figure 14 below.

https://doi.org/10.5194/egusphere-2026-2030
Preprint. Discussion started: 22 April 2026


## 3 Interpretation and model

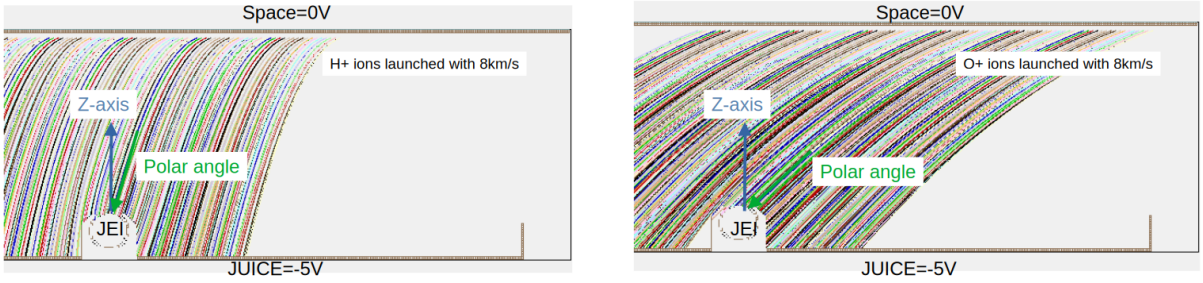


**Figure 12.** Simion simulation of the deflection of $H^+$ (left) and $O^+$ (right) ions in a linear spacecraft potential. Ions are launched with spacecraft velocity at 1 m distance in a linear potential with scale height 50 cm arriving at the instrument with different polar inclination angles $\theta$.

Figure 12 shows a Simion simulation of ion trajectories in a linear and planar potential of $V_p$ = –5V at spacecraft surface and instrument and 0V at 50 cm distance. Ions are launched parallel to the spacecraft surface at 50 cm distance with mass per charge of 1 amu/q(left) and 16 amu/q(right) and a velocity of $v_x$ = 8 km/s. One can see that the lighter ions reach the JEI sensor at a higher polar inclination angle than the heavy ions. To explain this we can calculate the polar inclination angle $\theta$ relative to the vertical axis for a planar potential by

$$\tan\theta = v_x/v_y = \frac{v_x}{\sqrt{qV_p/(2m)} + v_{y0}}, \tag{1}$$

where $(v_x, v_{y0})$ are the initial velocity components parallel and perpendicular to the spacecraft surface, $V_p$ is the spacecraft potential and $m/q$ is the ion mass per charge. The expected observed energy per charge is $E/q = 2m|v|^2 + V_p$. In Table 1 we calculate the expected mean inclination angles for different ion species for the conditions valid at around 21:50 UTC where the spectra shown in Figures 10 and 11 were observed. From Figure 6 we can read the approximate initial velocities either assuming that the plasma is at rest relative to Earth in the GSE frame or rotating with corotation speed. We here assume a spacecraft potential of –5.0V - slightly lower than the value reported by RPWI (Fig. 8). Since the initial polar inclination angle is about $45^o$ the expected inclination angle decreases with increasing potential. The maximum ion mass we consider is 32 amu/q ($O_2^+$). Earlier observations of heavy molecules in the plasmasphere (Craven et al., 1985) suggest that molecules with mass 28 and 30 amu/q ($N_2^+$ and $NO^+$) may be more abundant than $O_2^+$. The energy resolution of the JEI sensor does not allow to separate these masses such that $O_2^+$ is considered only as representative for the heavy molecular component. Similar spatial effects of the spacecraft potential on the ion distribution were discussed in context of the Rosetta mission (Nyffenegger et al., 2001; Bergman et al., 2020).

We can see from Figure 9 that ions are observed only for polar inclination angles smaller than $45^o$ in agreement with the expectation that the spacecraft potential decreases the inclination angle. We can also see that spectra observed at inclination angles $<25^o$ show only a single or double Maxwellian distributions as the example shown in Figure 10 (right panels). Table 1

https://doi.org/10.5194/egusphere-2026-2030
Preprint. Discussion started: 22 April 2026


| $\|v_x\|$ | $\|v_{y0}\|$ | $V_p$ | $\theta$ $H^+$ | $\theta$ $He^+$ | $\theta$ $He^{++}$ | $\theta$ $O^+$ | $\theta$ $O_2$+ | $E/Q$ $H^+$ | $E/Q$ $He^+$ | $E/Q$ $He^{++}$ | $E/Q$ $O^+$ | $E/Q$ $O_2$+ |
|---|---|---|---|---|---|---|---|---|---|---|---|---|
| 6.0 | 5.0 | –5.0 | 9.4$^o$ | 16.2$^o$ | 12.5$^o$ | 25.2$^o$ | 29.8$^o$ | 5.3 eV | 6.3 eV | 5.7 eV | 10.3 eV | 15.6 eV |
| 5.0 | 5.0 | –5.0 | 7.9$^o$ | 13.7$^o$ | 10.5$^o$ | 21.4$^o$ | 25.5$^o$ | 5.2 eV | 6.0 eV | 5.5 eV | 9.0 eV | 13.1 eV |
| 5.0 | 5.0 | –2.0 | 11.5$^o$ | 18.6$^o$ | 14.8$^o$ | 26.8$^o$ | 33.7$^o$ | 2.3 eV | 3.0 eV | 2.5 eV | 6.0 eV | 10.1 eV |

**Table 1.** Expected mean polar inclination angle $\theta$ relative to SC Z-axis for different initial velocities and SC potentials $V_p$.

shows that spectra observed at lower angles should be dominated by light ions - mainly $H^+$, $He^+$ and $He^{++}$. The high energy tail seen at $\theta = 14.4^o$ may be contributed by the helium ions. Only at inclination angles $>25^o$ we can see spectra with higher mean energy per charge and separate peaks in the spectrum as shown in Figure 11. We interprete these as being dominated by heavier ions. Since the peak with maximum energy per charge is observed at 15.0 eV we may conclude from the values shown in the table that:

1) the effective spacecraft potential at the location of the JEI sensor is probably around –5.0V about 1.5V less negative than the value reported by RPWI,

2) the heavy molecular component is predicted to have a mean energy per charge of 15.6eV and a predicted mean polar inclination angle of 29.8$^o$,

3) the smaller flux peaks observed at 5–7 eV/q are caused by the thermal spread of the light ion distribution,

4) the distribution observed between 8 and 13 eV/q can be associated with heavier ions. We can for example not exclude contributions by nitrogen ions.

To better quantify the contribution to the spectra shown in Figures 10 and 11 we made a sensor response calculation for the specific ion species and geometries listed in Table 1. We assume for all ions a common initial velocity of 7.5 km/s, an acceleration by a –5.0V potential, a temperature of 0.1 eV and a density of $n_0$ =1000/cm$^3$ for each species. We take the same density for each species to later allow a scaling to the observed count rate. We derive the expected phase space distribution for each species as a function of angular distance from the beam center as explained in Appendix B. From the phase space distribution we derive the particle flux using the base geometric factor given in Table A1. But here we also take the polar angle ($\theta$) dependence of the efficiency into account which reduces the geometric factor at smaller polar angles. We also include the dependence of the CEM efficiency on ion mass and pre-acceleration voltage (CEM_head) into account using the general formula for MCPs from Krems et al. (2005).

Figure 13 shows the expected counts in each energy bin for the inclination angles listed in the first line of Table 1. The integration time per energy bin is 3 ms . The plots divide the polar field-of-view of JEI (10$^o$–75$^o$) into 16 sectors of 4.4$^o$ width. The JEI sensor was operated during this observation pass with a division of the polar field-of-view into only 8 sectors, but the polar full width half maximum (FWHM) of the sensor for a cold beam is only about 5$^o$ such that only every second sector shown in Figure 13 was observed by JEI. The mean angles of the JEI polar sectors are given in Figures 10 and 11.

https://doi.org/10.5194/egusphere-2026-2030
Preprint. Discussion started: 22 April 2026


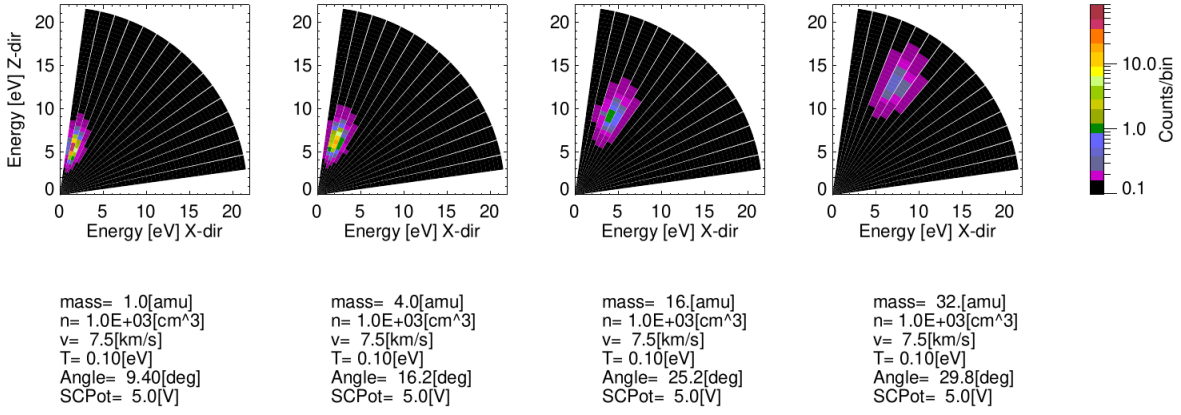


**Figure 13.** Instrument response calculation *including CEM efficiency* (Krems et al., 2005) for different ion species arriving under the polar inclination angles listed in the first line of Table 1 with acceleration of a –5.0V spacecraft potential. Ions shown from left to right are $H^+$, $He^+$, $O^+$ and $O_2^+$. We assume for this simulation an initial density of 1000.0/$cm^3$ (in spacecraft frame) per species and an initial velocity of 7.5 km/s. Shown are the expected counts in each measurement interval of 3 ms per energy bin.

https://doi.org/10.5194/egusphere-2026-2030
Preprint. Discussion started: 22 April 2026


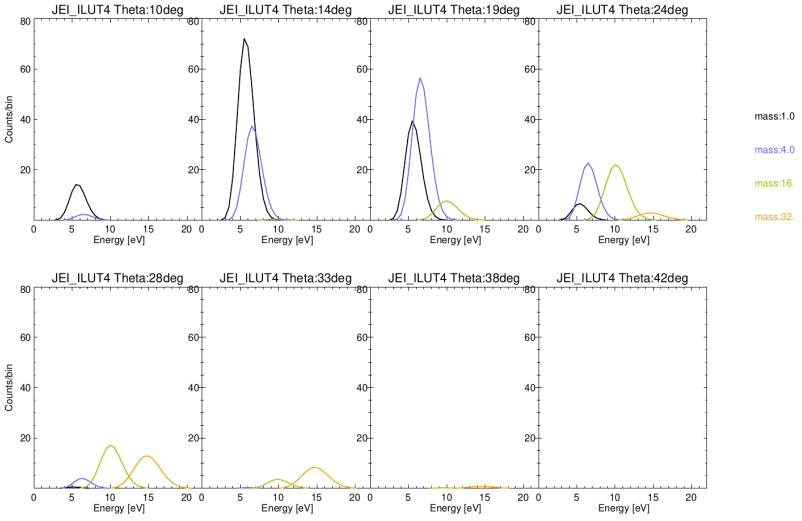


**Figure 14.** Same simulation setup as for Figure 13 showing the simulated contribution of different ion species [H+ (black line), He+ (blue line), O+ (green line) and O2+ (orange line)] of same density to the observed count spectra for the upper 8 virtual polar inclination angles (listed on top).

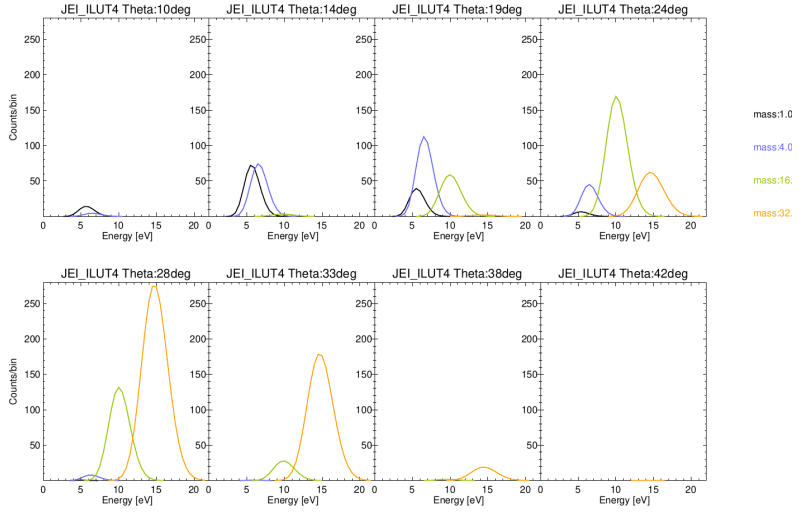


**Figure 15.** Same simulation setup as in Figure 14 *but with $H^+$ CEM efficiency for all ions* showing the simulated contribution of different ion species of same density to the observed count spectra for the upper 8 virtual polar inclination angles (listed on top).

https://doi.org/10.5194/egusphere-2026-2030
Preprint. Discussion started: 22 April 2026


In Figure 14 we overlayed the predicted contributions of the different ion species to the spectrum observed under the top 8 polar simulation sectors - only 4 of these sectors have been observed by the JEI sensor. These distributions can now be compared with the 4 observed spectra shown in Figures 10 and 11. Note, that the simulation uses the same density of $1000.0/\mathrm{cm}^3$ for each species. We can see that the spectrum observed at $14.4^o$ can have contributions of $H^+$ and $He^+$ where the density of $177 \pm 45/\mathrm{cm}^3$ obtained by fitting shown in Figure 10 can not be directly compared because is does not contain the dependence of the efficiency on elevation angle and pre-acceleration voltage of the sensor. To obtain a more realistic density value for $H^+$ (assuming that $He^+$ is minor) we may multiply the assumed density $n_0$ by the ratio of the peak counts in Figure 10 and Figure 14 for the respective $\theta$ angles. We then get:

$$\begin{aligned}
\theta = 14^o : n_{H^+} = &\quad n_0 * (100.0 \pm 10)/70.0 = 1430 \pm 140/\mathrm{cm}^3, \\
\theta = 19^o - 24^o : n_{He^+} = &\quad n_0 * (80.0 \pm 9)/60.0 = 1330 \pm 150/\mathrm{cm}^3, \\
\theta = 28^o - 33^o : n_{O^+} = &\quad n_0 * (65.0 \pm 8)/20.0 = 3250 \pm 400/\mathrm{cm}^3, \\
\theta = 28^o - 33^o : n_{O_2^+} = &\quad n_0 * (60.0 \pm 8)/15.0 = 4000 \pm 530/\mathrm{cm}^3.
\end{aligned} \tag{2}$$

The errors shown contain just the error of the counting statistics, but there are several other possible sources of error in these estimations such as: value of spacecraft potential, corotation speed of plasmasphere, polar angle response of the geometric factor, CEM efficiency dependence on mass and energy. Especially the latter may lead to an overestimate of the heavy ion densities. For this reason we repeated the calculation by assuming the efficiency of $H^+$ for all ions as shown in Figure 15. One can see that this makes a significant difference. If we now calculate densities based on this response assumption we get:

$$\begin{aligned}
\theta = 14^o : n_{H^+} = &\quad n_0 * (100.0 \pm 10)/70.0 = 1430 \pm 140/\mathrm{cm}^3, \\
\theta = 19^o - 24^o : n_{He^+} = &\quad n_0 * (80.0 \pm 9)/60.0 = 660 \pm 80/\mathrm{cm}^3, \\
\theta = 28^o - 33^o : n_{O^+} = &\quad n_0 * (65.0 \pm 8)/20.0 = 460 \pm 60/\mathrm{cm}^3, \\
\theta = 28^o - 33^o : n_{O_2^+} = &\quad n_0 * (60.0 \pm 8)/15.0 = 220 \pm 30/\mathrm{cm}^3.
\end{aligned} \tag{3}$$

This comparison shows the significant influence of the CEM efficiency on the calibration for heavy ions. Unfortunately the JEI sensor operated during the observation with a rather low post-acceleration voltage *CEM_head* of –250V which does not provide enough acceleration for heavy ions. The nominal post-acceleration for observations at Jupiter in ion mode is –1000V but for safety reasons this was not applied during the JEI operations during the LEGA. To solidify the quantitative density estimates for these observations laboratory tests of the CEM efficiency at –250V post-acceleration are needed. In 2017 ion beam tests of the JEI CEMs were done at –370V total ion energy with $H_2^+$ and $N_2^+$ ions. These showed that the efficiency of the heavier ions was smaller than for the light ions by a factor of only ∼0.8 (I. Szemerey, personal communication). The respective ratio for this energy returned by the MCP formula of Krems et al. (2005) is ∼0.1. This indicates that the assumption of a mass independent efficiency can be more realistic for the JEI CEMs. In addition to these considerations a specific correction of the observed densities taking into account the shape of the spacecraft potential may be applied as explained in Appendix C. But this correction is expected to be small compared to the influence of the CEM efficiency.

https://doi.org/10.5194/egusphere-2026-2030
Preprint. Discussion started: 22 April 2026


Nevertheless the simulation shows that the heavy ion contribution to the total density during the JUICE plasmasphere passage is at least 30%. Additionally, the spectral peak at 15 $\mathrm{eV/q}$ is difficult to explain without considering molecular heavy ions.

## 4 Discussion

The negative charging of the JUICE spacecraft allowed a rare direct measurement of the plasmaspheric cold ion distribution by the PEP JEI electrostatic analyzer. This is a novel measurement as compared to the multiple observations by RPA instruments flown in the earlier phases of magnetospheric science. The advantage of the electrostatic analyzer is a rather high energy and spatial resolution as compared to RPA instruments. More recent missions (Cluster, MMS, Van-Allen-Probe) used electrostatic analyzers but were inhibited by tuning of the instruments to higher energies or by positive charging of the spacecraft. The PEP JEI sensor is a pure energy analyzer and has no built-in mass discrimination. As we have demonstrated above the high spatial resolution of the sensor allows to use the negative spacecraft potential as a mass filter for cold ions when they have a common bulk speed determined by the spacecraft velocity. The location of the flux peak for $H^+$ and $He^+$ are with 5.2 eV and 5.6 eV lower than expected for a spacecraft potential of –6.5V as measured by RPWI. The reason may either lie in a difference between spacecraft ground and JEI electronics ground or a potential deviation at the specific location of the JEI sensor (Zeroual et al., 2026). In our calculations we assume a value of –5.0V for the potential.

One topic we have not yet discussed is the influence of the magnetic field on the observations. Observations in the outer plasmasphere ($L > 3R_E$) indicate in addition to the cold ion distribution a significant warm ion distribution with temperature > 1 eV and mean energy > 10 eV (Goldstein et al., 2023). As shown in Figure 6 the predicted magnetic field polar angle coincides approximately with the spacecraft velocity vector. This could suggest that the more energetic ion population observed by JEI may also be interpreted as a field-aligned energized proton distribution. But this would not explain the peaks in the spectrum which coincide with the modeled location for the different ion masses. Also the azimuthal angle $\phi$ of the predicted magnetic field is at $90^o$ (Figure 6), while the observed azimuth is in the range $–20^o$ to $+20^o$.

The flux peak observed in the energy spectrum around 15 eV (Fig. 11) indicates the presence of heavy molecular ions in the mass range 30–32 $\mathrm{amu/q}$. The steep fall off above 15 eV indicates that no heavier molecules than mass 32 $\mathrm{amu/q}$ are present. Since the efficiency of the JEI CEMs at the very low post-acceleration voltage of –250 V is not well known further calibrations are needed to quantify the relative contributions of the different ion species to the observed spectra.

The observed ion temperatures (Figure 10) should in principle not depend on the spacecraft potential when the negative potential is lower than the undisturbed minimum energy for a specific ion species. But this is not the case for the spectra observed at $\theta$=14.4$^o$ and $\theta$=23.8$^o$ where the observed mean energy is very close to the spacecraft potential reported by the RPWI instrument. In this case the part of the spectrum which is lower than the spacecraft potential will be accumulated in a single energy bin and the Maxwellian fit in energy space results in too low temperatures. This can explain that the temperature values reported in Figure 10 are lower than those obtained by earlier measurements using RPA instruments (Kotova et al., 2008).

https://doi.org/10.5194/egusphere-2026-2030
Preprint. Discussion started: 22 April 2026


## 5 Conclusions

During the first gravity assist of JUICE at Earth on 20th August 2024 the spacecraft passed through the Earth plasmasphere for about 2 hours. Before closest approach at a distance of 2.1 $R_E$ the Jovian Electron and Ion spectrometer (JEI) of the PEP instrument suite was switched on for 40min in an ion mode test configuration. The high plasma density of about 3000/$\mathrm{cm}^3$, as observed by the RPWI plasma wave instrument, led to a negative charging of the spacecraft which allowed a rare observation of the cold and dense plasmaspheric ion population. Since the ions are only corotating with the Earth with a velocity of about 1 $\mathrm{km/s}$ at this distance the observed ion speed is dominated by the spacecraft velocity of about 8 $\mathrm{km/s}$. For this reason ions with different masses are separating in the energy spectrum observed by JEI. In addition the spacecraft potential leads to specific filtering of ion masses in the observed angular distribution. By calculating the sensor response function for this specific geometry it is possible to quantify densities of the different ion species. This response calculation depends critically on the response of the JEI CEMs to the ion velocity and mass. Since the sensor was operated with a low post-acceleration, further laboratory calibrations may be needed for this specific setup. Still we can already conclude from the observations that ions with mass $> 4$ $\mathrm{amu/q}$ contribute at least 30% to the observed total density. A flux peak observed in the energy spectrum at 15 $\mathrm{eV/q}$ can only be explained by the presence of heavy molecular ions with mass $\sim$30 $\mathrm{amu/q}$. Molecular ions have only been rarely detected in the outer Earth plasmasphere. With respect to the performance and operations of PEP JEI, these observations show that PEP JEI can achieve sensitive ion composition measurements in the exospheres of the moons of Jupiter. A negative spacecraft potential in the Jovian plasma environment was also observed by the PLS instrument on the Galileo spacecraft (Frank and Paterson, 2000). This is supported by predictions of a negative spacecraft potential for JUICE (Bochet et al., 2023).

*Data availability.* Data of the PEP JEI sensor used in this study will be made available via the ESA PSA guest archive.

https://doi.org/10.5194/egusphere-2026-2030
Preprint. Discussion started: 22 April 2026


## Appendix A: JEI sensor properties

| Parameter | Value | Comment |
|---|---|---|
| Particles | Electrons and ions | alternating every 4.5s |
| Energy Range | 1 eV/q – 60 keV/q | nominal,by design |
| | 1 eV/q – 10 keV/q | during LEGA |
| | 100 eV/q – 17 keV/q | calibration range |
| Polar Range | $8^o$ – $78^o$ | up to 17 keV/q |
| | $30^o$ – $60^o$ | up to 60 keV/q |
| Polar resolution | $4.7^o$ – $6.0^o$ | depending on elevation |
| Azimuth range | $360^o$ | |
| Azimuth resolution | $22.5^o$ – $45.0^o$ | depending on elevation |
| Geometric factor | 3.0x10$^{-5}$cm$^2$ ssreV/eV | isotropic per anode |
| | | depending on elevation and mass/q |
| Analyzer constant k | 19.75 | Energy = k/2 * analyzer voltage |
| Maximum voltage | ±3000V | |
| Time resolution | 4 ms – 100 ms | per energy step, adjustable |
| | 4096 ms | 3d scan at 8x128 energy steps |
| Maximum count rate | 1 MHz | per anode |
| Sensor mass | 1.35kg/3.13kg | without/with shielding |
| Electronic mass | 0.672g | without shielding |
| Power consumption | 3.35W – 5.46 W | 4 – 16 channels |

**Table A1.** General properties of the PEP JEI sensor. Performance parameters will be updated during the JUICE inflight calibration campaign.

https://doi.org/10.5194/egusphere-2026-2030
Preprint. Discussion started: 22 April 2026


## Appendix B: The PEP JEI particle distribution function

The PEP JEI sensor is an electro-static particle analyzer using electro-static deflectors (Barabash, 2026; Bambach, 2026). This means at a given time step $\tau_s$ (=4 ms in the case discussed here) the sensor counts ions or electrons with a specific mean energy $E_m$ and energy distribution with a FWHM $\Delta E$ coming from a specific polar direction $\theta$ with a polar FWHM $\Delta\theta \approx 5^o$. The actual energy and polar width are dependent on $\theta$ (see Bambach (2026)).

JEI sweeps the energy analyzer and deflector voltages in parallel in 128 steps such that one energy spectrum is obtained within 512 ms from a specific polar direction $\theta$. The polar hemisphere is stepped through by 8 polar steps in the range $10^o$ to $75^o$ measured from the sensor symmetry axis. This means specifically for cold plasma distributions polar directions between each polar step may not be covered in this operation mode. The azimuth field of view is sampled simultaneously by the 16 anodes of the sensor. But since efficiency and noise background of each anode are different we here consider only one specific azimuth sector $\phi$ with its width $\Delta\phi$. In summary the sensor samples counts $c(E,\phi,\theta)$ from a specific viewing direction at a given time within the sampling period $\tau = \tau_s - -d$, where $d$=1 ms is the dead time between each energy step. The differential energy flux can be obtained from the count rate by (Fränz et al., 2006):

$$J_E(E,\phi,\theta) = \frac{c(E,\phi,\theta)}{G_E \tau} \tag{B1}$$

where $G_E$ is the energy geometric factor which is assumed to be constant over the low energy interval under discussion. The partial phase space density for a given plasma component with mass $m$ and velocity $\boldsymbol{v}$ is then given by

$$f(\boldsymbol{v}) = \frac{m^2 \cdot J_E(E,\phi,\theta)}{2E^2} \tag{B2}$$

where $\boldsymbol{v} = \sqrt{2E/m} \cdot \boldsymbol{n}$ and $\boldsymbol{n} = (\sin\theta\cos\phi, \sin\theta\sin\phi, \cos\theta)$ is the vector opposite to the viewing direction.

The energy geometric factor of JEI for an isotropic distribution is given in Table A1. The factor is larger for a mono-directional flow when looking into flow direction and needs to be modeled for each case.

To derive the expected energy flux for a given Maxwellian plasma flow with density $n$, mean velocity $\bar{\boldsymbol{v}}$ and thermal velocity $v_t$ we can use its phase space density distribution:

$$f(\boldsymbol{v}) = \frac{n}{(\sqrt{\pi} v_t)^3} \cdot \exp - \frac{(\bar{\boldsymbol{v}} - \boldsymbol{v})^2}{v_t^2} \tag{B3}$$

To use angular coordinates we can replace the vector coordinates by

$$f(\boldsymbol{v}) = \frac{n}{(\sqrt{\pi} v_t)^3} \cdot \exp - \frac{\bar{v}^2 - 2\bar{v}|v|\cos\Delta\sigma + v^2}{v_t^2} \tag{B4}$$

where $\Delta\sigma$ is the distance between viewing direction $(\phi,\theta)$ and mean flow direction $(\phi_f,\theta_f)$ along the great circle (all angles in radian):

$$\Delta\sigma = \arccos(\sin\theta\sin\theta_f + \cos\theta\cos\theta_f\cos|\phi - \phi_f|) \tag{B5}$$

If we replace the thermal velocity $v_t$ by thermal energy $E_t$ and the mean velocity by mean energy $\bar{E}$ we get

$$f(\boldsymbol{v}) = n \cdot (\frac{m}{\pi 2 E_t})^{3/2} \cdot \exp - \frac{\bar{E} - 2\sqrt{\bar{E}E}\cos\Delta\sigma + E^2}{E_t} \tag{B6}$$

https://doi.org/10.5194/egusphere-2026-2030
Preprint. Discussion started: 22 April 2026


This generalizes equation 18 of Fränz et al. (2006) which is only valid for $\Delta\sigma = 0$.

If we now consider an anode looking in flow direction (that is receiving the peak signal) we can assume $\phi = \phi_f$. In this case we get

$$\cos\Delta\sigma = \sin\theta\sin\theta_f + \cos\theta\cos\theta_f = \cos(\theta - \theta_f) \tag{B7}$$

340 Using equations B3 and B6 we can thus determine for an assumed Maxwellian plasma flow the expected energy flux in each angular direction and energy bin of the sensor.

https://doi.org/10.5194/egusphere-2026-2030
Preprint. Discussion started: 22 April 2026


## Appendix C: Density correction in a planar potential

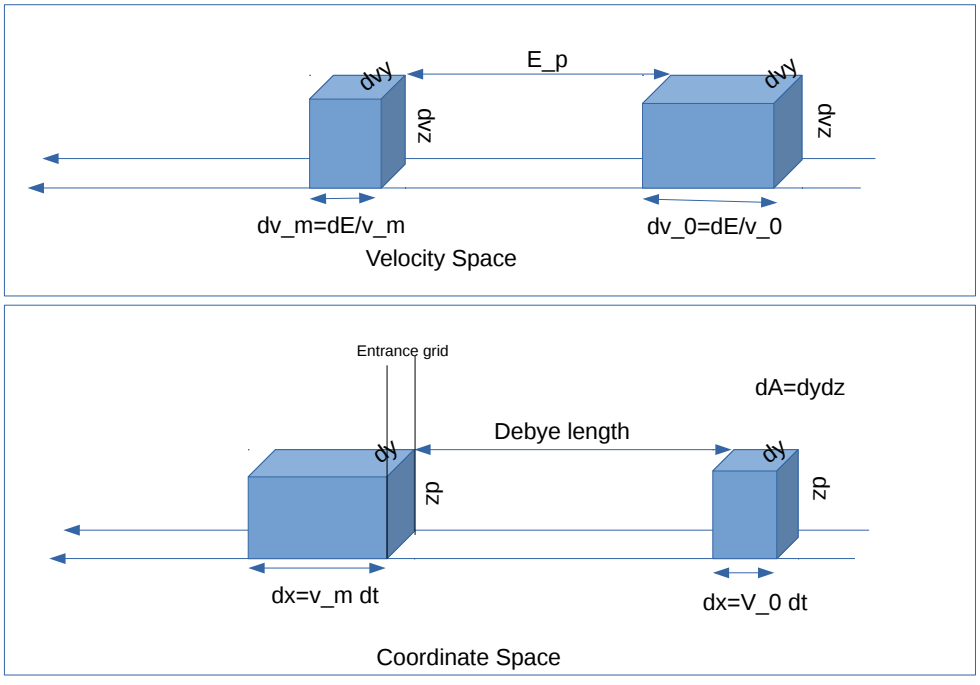


**Figure A1.** Planar geometry of acceleration by potential in velocity and coordinate space. The size of the phase space volume element does not change. Flux through surface dA is conserved.

The effect of electric potentials on the plasma flow was already analyzed in much detail in the seminal paper by Mott-Smith and Langmuir (1926) in the context of plasma probes. For convenience in the following we describe the derivation in planar geometry since the more recent papers usually assume spherical geometry. We generally assume that the spacecraft is located in a mono-directional plasma flow with density $n_0$ and velocity $v_0$. If the ion sensor is located behind a planar entrance grid and the flow is perpendicular to this grid we are dealing with a one-dimensional problem as shown in Figure A1. Liouville's theorem in general form states that the phase space density of particles $S = dN/dV$ in a volume element $dV$ of phase space is conserved along the flow, in cartesian geometry:

$$S dv_x dv_y dv_z dx dy dz = dN \tag{A1}$$

where $dN$ denotes the number of particles and $dV = dv_x dv_y dv_z dx dy dz$ the size of the volume element. In 1D geometry this reduces to $\frac{dN}{dvdx} = constant$ since $dv_y dv_z dy dz$ is constant. Now, the quantity measured by ion sensors is the flux of ions $F$ with mean energy $E$ crossing an area $dA$ perpendicular to the flow direction in a given time $dt$ for a given energy interval $dE$.

https://doi.org/10.5194/egusphere-2026-2030
Preprint. Discussion started: 22 April 2026


In 1D the spatial extent of the volume element along the flow is given by $dx = vdt$ and since $dE = vdv$ we have

$$Sdvdx = S\frac{dE}{v}vdt = SdEdt \propto dN \tag{A2}$$

The particle number flux of particles crossing a given area $dA$ in a given time $dt$ is given by $F = dN/dAdt \sim SdE$. Liouville's theorem in 1D then states $F/dE$ is constant. Thus if an instrument measures with the same energy width $dE$ outside of the potential or inside of the potential it will measure the same particle number flux - only at a different energy. From $E_m = E_0 + E_p$ it follows also that $dE_m = dE_0$. We again stress that if a sensor measures with a geometric factor which depends on energy it is irrelevant for this discussion because this happens behind the entrance grid of the sensor. Outside of the potential the number flux is given by $F = n_0 v_0$, since the mean velocity $v_m$ measured inside of a potential $E_p$ is given by $v_m = \sqrt{v_0^2 + sv_p^2}$, where $v_p = \sqrt{|E_p|/2m}$ and $s = --\text{sign}(E_p)$, the observed ion density $n_m$ is given by

$$n_m = \frac{n_0 v_0}{\sqrt{v_0 + sv_p}} = \frac{n_0}{\sqrt{1 + s(\frac{v_p}{v_0})^2}} = \frac{n_0}{R_v} \tag{A3}$$

where we define the *velocity ratio* $R_v = \sqrt{1 + s(\frac{v_p}{v_0})^2}$. That means the observed density is lower than the undisturbed density $n_0$ for a negative potential. We note that this is different from the usual correction for potentials with a spherical geometry where the potential focuses the flux (Lavraud and Larson, 2016).

*Author contributions.* The data analysis was performed by Markus Fränz, Elias Roussos, and Jan-Erik Wahlund. Henning Fischer is the lead engineer of the JEI sensor. Other co-authors supervise build and operation of JUICE PEP and provided corrections to the analysis.

*Competing interests.* At least one of the (co-)authors is a member of the editorial board of Annales Geophysicae.

*Acknowledgements.* JUICE is a mission under ESA leadership with contributions from its Member States, NASA, JAXA, and the Israel Space Agency. It is the first Large-class mission in ESA's Cosmic Vision programme. The JUICE/RPWI instrument is supported by the Swedish National Space Agency (SNSA). The German contribution to the PEP instrument suite and its operation was and is being funded by the German Federal Ministry for Economic Affairs and Climate Action / German Federal Ministry of Research, Technology and Space (BMFTR) through the German Space Agency at DLR on the basis of a resolution of the German Bundestag (Funding codes: 50QJ1301, 50QJ1503 and 50QJ2303) and by the Max Planck Society. This publication has emanated from research conducted with the financial support of Taighde Éireann - Research Ireland under Grant number [22/PATH-S/10757], awarded to MKGH. French co-authors acknowledge the support of CNES for the Juice mission. We also thank Susan McKenna-Lawlor of the Maynooth University, Ireland, for supporting the PEP instrument development.

https://doi.org/10.5194/egusphere-2026-2030
Preprint. Discussion started: 22 April 2026


## References

Bambach, P.: Calibration of the JEI sensor for the JUICE spacecraft, Ph.D. thesis, University of Stuttgart, 2026.

Barabash, S.: Particle Environment Package (PEP) for the JUICE mission, Space Sci.Rev., 2026.

Bergman, S., Stenberg Wieser, G., Wieser, M., Johansson, F. L., and Eriksson, A.: The Influence of Varying Spacecraft Potentials and Debye Lengths on In Situ Low-Energy Ion Measurements, Journal of Geophysical Research: Space Physics, 125, e2020JA027 870, https://doi.org/https://doi.org/10.1029/2020JA027870, e2020JA027870 2020JA027870, 2020.

Bochet, M., Bergman, S., Holmberg, M. K. G., Wieser, M., Wieser, G. S., Wittmann, P., Gourinat, Y., Imhof, C., and Barabash, S.: Perturbations of JUICE/JDC Ion Measurements Caused by Spacecraft Charging in the Jovian Magnetosphere and the Ionosphere of Ganymede, Journal of Geophysical Research: Space Physics, 128, e2023JA031 377, https://doi.org/https://doi.org/10.1029/2023JA031377, e2023JA031377 2023JA031377, 2023.

Chappell, C. R., Fields, S. A., Baugher, C. R., Hoffman, J. H., Hanson, W. B., Wright, W. W., Hammack, H. D., Carignan, G. R., and Nagy, A. F.: The Retarding Ion Mass Spectrometer on Dynamics Explorer-A., Space Science Instrumentation, 5, 477–491, 1981.

Comfort, R. H.: Thermal structure of the plasmasphere, Advances in Space Research, 17, 175–184, https://doi.org/10.1016/0273-1177(95)00710-V, 1996.

Comfort, R. H., Waite, Jr., J. H., and Chappell, C. R.: Thermal ion temperatures from the retarding ion mass spectrometer on DE 1, Journal of Geophysical Research: Space Physics, 90, 3475–3486, https://doi.org/10.1029/JA090iA04p03475, 1985.

Craven, P. D., Olsen, R. C., Chappell, C. R., and Kakani, L.: Observations of molecular ions in the earth's magnetosphere, Journal of Geophysical Research: Space Physics, 90, 7599–7606, https://doi.org/10.1029/JA090iA08p07599, 1985.

Darrouzet, F., de Keyser, J., and Pierrard, V.: The Earth's Plasmasphere, https://doi.org/10.1007/978-1-4419-1323-4, 2009.

Delzanno, G. L., Borovsky, J. E., Henderson, M. G., Resendiz Lira, P. A., Roytershteyn, V., and Welling, D. T.: The impact of cold electrons and cold ions in magnetospheric physics, Journal of Atmospheric and Solar-Terrestrial Physics, 220, 105 599, https://doi.org/https://doi.org/10.1016/j.jastp.2021.105599, 2021.

Frank, L. A. and Paterson, W. R.: Observations of plasmas in the Io torus with the Galileo spacecraft, Journal of Geophysical Research: Space Physics, 105, 16 017–16 034, https://doi.org/https://doi.org/10.1029/1999JA000250, 2000.

Fränz, M., Dubinin, E., Roussos, E., Woch, J., Winningham, J. D., Frahm, R., Coates, A. J., Fedorov, A., Barabash, S., and Lundin, R.: Plasma Moments in the Environment of Mars. Mars Express ASPERA-3 Observations, Space Science Review, 126, 165–207, https://doi.org/10.1007/s11214-006-9115-9, 2006.

Fränz, M., Bührke, U., Ferreira, P., Fischer, H., Heumüller, P., Krupp, N., Kühne, W., and Roussos, E.: The Jovian Electron and Ion Spectrometer (JEI) for the JUICE mission, in: European Planetary Science Congress, pp. EPSC2017–464, 2017.

Gallagher, D. L., Craven, P. D., and Comfort, R. H.: Global core plasma model, Journal of Geophysical Research (Space Physics), 105, 18,819–18,833, https://doi.org/10.1029/1999JA000241, 2000.

Genestreti, K. J., Goldstein, J., Corley, G. D., Farner, W., Kistler, L. M., Larsen, B. A., Mouikis, C. G., Ramnarace, C., Skoug, R. M., and Turner, N. E.: Temperature of the plasmasphere from Van Allen Probes HOPE, Journal of Geophysical Research: Space Physics, 122, 310–323, https://doi.org/https://doi.org/10.1002/2016JA023047, 2017.

Goldstein, J., Chappell, C. R., Davis, M. W., Denton, M. H., Denton, R. E., Gallagher, D. L., Gladstone, G. R., Lecocke, M. B., Sandel, B. R., and Windt, D. L.: Imaging the Global Distribution of Plasmaspheric Oxygen, Journal of Geophysical Research (Space Physics), 123, 2078–2103, https://doi.org/10.1002/2017JA024531, 2018.

https://doi.org/10.5194/egusphere-2026-2030
Preprint. Discussion started: 22 April 2026


Goldstein, J., Burch, J. L., Fuselier, S. A., Gomez, R., Gonzalez, C. A., Kim, M. J., Mukherjee, J., Turner, N. E., and Wilson, M. E.: MMS Observations of Dayside Warm (Several eV to 100 eV) Ions in the Middle and Outer Magnetosphere, Journal of Geophysical Research: Space Physics, 128, e2022JA031 051, https://doi.org/https://doi.org/10.1029/2022JA031051, e2022JA031051 2022JA031051, 2023.

Grasset, O., Dougherty, M. K., Coustenis, A., Bunce, E. J., Erd, C., Titov, D., Blanc, M., Coates, A., Drossart, P., Fletcher, L. N., Hussmann, H., Jaumann, R., Krupp, N., Lebreton, J.-P., Prieto-Ballesteros, O., Tortora, P., Tosi, F., and Van Hoolst, T.: JUpiter ICy moons Explorer (JUICE): An ESA mission to orbit Ganymede and to characterise the Jupiter system, Planentary and Space Science, 78, 1–21, https://doi.org/10.1016/j.pss.2012.12.002, 2013.

Gringauz, K. I.: Plasmasphere and its interaction with the ring current., Space Science Rev., 34, 245–257, https://doi.org/10.1007/BF00175281, 1983.

Hoffman, J. H., Dodson, W. H., Lippincott, C. R., and Hammack, H. D.: Initial ion composition results from the Isis 2 satellite, Journal of Geophysical Research (Space Physics), 79, 4246, https://doi.org/10.1029/JA079i028p04246, 1974.

Jahn, J.-M., Goldstein, J., Kurth, W. S., Thaller, S., De Pascuale, S., Wygant, J., Reeves, G. D., and Spence, H. E.: Determining Plasmaspheric Density From the Upper Hybrid Resonance and From the Spacecraft Potential: How Do They Compare?, Journal of Geophysical Research: Space Physics, 125, e2019JA026 860, https://doi.org/https://doi.org/10.1029/2019JA026860, e2019JA026860 10.1029/2019JA026860, 2020.

James, M. K., Yeoman, T. K., Jones, P., Sandhu, J. K., and Goldstein, J.: The Scalable Plasma Ion Composition and Electron Density (SPICED) Model for Earth's Inner Magnetosphere, Journal of Geophysical Research: Space Physics, 126, e2021JA029 565, https://doi.org/https://doi.org/10.1029/2021JA029565, e2021JA029565 2021JA029565, 2021.

Kotova, G., Bezrukikh, V., Verigin, M., and Smilauer, J.: New aspects in plasmaspheric ion temperature variations from INTERBALL 2 and MAGION 5 measurements, Journal of Atmospheric and Solar-Terrestrial Physics, 70, 399–406, https://doi.org/https://doi.org/10.1016/j.jastp.2007.08.054, recent Observations and Simulations of the Sun-Earth System, 2008.

Krems, M., Zirbel, J., Thomason, M., and DuBois, R. D.: Channel electron multiplier and channelplate efficiencies for detecting positive ions, Review of Scientific Instruments, 76, 093305-093305-7, https://doi.org/10.1063/1.2052052, 2005.

Larsen, B. A., Klumpar, D. M., and Gurgiolo, C.: Correlation between plasmapause position and solar wind parameters, Journal of Atmospheric and Solar-Terrestrial Physics, 69, 334–340, https://doi.org/10.1016/j.jastp.2006.06.017, 2007.

Lavraud, B. and Larson, D. E.: Correcting moments of in situ particle distribution functions for spacecraft electrostatic charging, Journal of Geophysical Research (Space Physics), 121, 8462–8474, https://doi.org/10.1002/2016JA022591, 2016.

Lejosne, S., Maus, S., and Mozer, F. S.: Model-observation comparison for the geographic variability of the plasma electric drift in the Earth's innermost magnetosphere, Geophysical Res.Letts., 44, 7634–7642, https://doi.org/10.1002/2017GL074862, 2017.

Lin, M.-Y. and Ilie, R.: A review of observations of molecular ions in the Earth's magnetosphere-ionosphere system, Frontiers in Astronomy and Space Sciences, 8, 223, https://doi.org/10.3389/fspas.2021.745357, 2022.

Lu, J. Y., Zhou, Y., Ma, X., Wang, M., Kabin, K., and Yuan, H. Z.: Earth's Bow Shock: A New Three-Dimensional Asymmetric Model With Dipole Tilt Effects, Journal of Geophysical Research (Space Physics), 124, 5396–5407, https://doi.org/10.1029/2018JA026144, 2019.

Maldonado, C. A., Resendiz Lira, P. A., Delzanno, G. L., Larsen, B. A., Reisenfeld, D. B., and Coffey, V.: A review of instrument techniques to measure magnetospheric cold electrons and ions, Frontiers in Astronomy and Space Sciences, Volume 9 - 2022, https://doi.org/10.3389/fspas.2022.1005845, 2023.

Mott-Smith, H. M. and Langmuir, I.: The Theory of Collectors in Gaseous Discharges, Physical Review, 28, 727–763, https://doi.org/10.1103/PhysRev.28.727, 1926.

https://doi.org/10.5194/egusphere-2026-2030
Preprint. Discussion started: 22 April 2026


Nyffenegger, O., Mildner, M., Wurz, P., Altwegg, K., Balsiger, H., and Berthelier, J. J.: Influence of Electric Charging on the ROSINA Instrument in the Plasma Environment of Comet 46P/Wirtanen, in: Spacecraft Charging Technology, edited by Harris, R. A., vol. 476 of *ESA Special Publication*, p. 203, 2001.

Roberts, Jr., W. T., Horwitz, J. L., Comfort, R. H., Chappell, C. R., Waite, Jr., J. H., and Green, J. L.: Heavy ion density enhancements in the outer plasmasphere, Journal of Geophysical Research (Space Physics), 92, 13 499–13 512, https://doi.org/10.1029/JA092iA12p13499, 1987.

Sauvaud, J.-A., Lundin, R., Rème, H., McFadden, J. P., Carlson, C., Parks, G. K., Möbius, E., Kistler, L. M., Klecker, B., Amata, E., DiLellis, A. M., Formisano, V., Bosqued, J. M., Dandouras, I., Décréau, P., Dunlop, M., Eliasson, L., Korth, A., Lavraud, B., and McCarthy, M.: Intermittent thermal plasma acceleration linked to sporadic motions of the magnetopause, first Cluster results, Annales Geophysicae, 19, 1523–1532, https://doi.org/10.5194/angeo-19-1523-2001, 2001.

Shue, J.-H., Song, P., Russell, C. T., Steinberg, J. T., Chao, J. K., Zastenker, G., Vaisberg, O. L., Kokubun, S., Singer, H. J., Detman, T. R., and Kawano, H.: Magnetopause location under extreme solar wind conditions, Journal of Geophysical Research (Space Physics), 103, 17 691–17 700, https://doi.org/10.1029/98JA01103, 1998.

Stenberg Wieser, G., Wieser, M., Barabash, S., Wittmann, P., and Wahlund, J.-E.: Flying through the plasmasphere to optimize low energy ion measurements, Annales Geophysicae, 2026.

Tsyganenko, N. A. and Stern, D. P.: Modeling the global magnetic field of the large-scale Birkeland current systems, Journal of Geophysical Research (Space Physics), 101, 27 187–27 198, https://doi.org/10.1029/96JA02735, 1996.

Wahlund, J.-E., Bergman, J. E. S., Åhlén, L., Puccio, W., Cecconi, B., Kasaba, Y., Müller-Wodarg, I., Rothkaehl, H., Morawski, M., Santolik, O., Soucek, J., Grygorczuk, J., Wisniewski, Ł., Henri, P., Rauch, J. L., Le Duff, O., Retinò, A., Mansour, M., Stverak, S., Laifr, J., Andrews, D., André, M., Benko, I., Berglund, M., Cripps, V., Cully, C., Davidsson, J., Dimmock, A., Edberg, N. J. T., Eriksson, A. I., Fredriksson, J., Gill, R., Gomis, S., Holback, B., Jansson, S.-E., Johansson, F., Johansson, E. P. G., Khotyaintsev, Y., Mårtensson, B., Morooka, M. W., Nilsson, T., Ohlsson, D., Pelikan, D., Richard, L., Shiwa, F., Vigren, E., Wong, H. C., Bonnin, X., Girard, J. N., Grosset, L., Henry, F., Lamy, L., Lebreton, J.-P., Zarka, P., Katoh, Y., Kita, H., Kumamoto, A., Misawa, H., Tsuchiya, F., Galand, M., Barcinski, T., Baran, J., Kowalski, T., Szewczyk, P., Grison, B., Jansky, J., Kolmasova, I., Lan, R., Pisa, D., Taubenschuss, U., Uhlir, L., Bochra, K., Borys, M., Duda, M., Kucinski, T., Ossowski, M., Palma, P., Tokarz, M., Colin, F., Dazzi, P., De Léon, E., Hachemi, T., Millet, A.-L., Randrianboarisson, O., Sene, O., Chust, T., Le Contel, O., Canu, P., Hadid, L., Sahraoui, F., Zouganelis, Y., Alison, D., Ba, N., Jeandet, A., Lebassard, M., Techer, J.-D., Mehrez, F., Varizat, L., Sumant, A. V., Sou, G., Hellinger, P., Travnicek, P., Bylander, L., Giono, G., Ivchenko, N., Kullen, A., Roth, L., Vaivads, A., Tanimoto, K., Mizuno, H., Sawamura, A., Suzuki, T., Namiki, M., Fujishima, S., Asai, K., Shimoyama, T., Fujii, M., Sato, Y., Birch, J., Bakhit, B., Greczynski, G., Gare, P., Landström, S., LeLetty, R., Ryszawa, E., Torralba, I., Trescastro, J. L., Osipenco, S., Wiklund, U., Roos, A., Söderström, J. C., Björneholm, O., Fischer, G., Nyberg, T., Kovi, K. K., Balikhin, M., Yearby, K. H., Holmberg, M., Jackman, C. M., Louis, C. K., Rhouni, A., Leray, V., Geyskens, N., Berthod, C., Lemaire, B., Clémencon, A., Wattieaux, G., André, N., Garnier, P., Génot, V., Louarn, P., Marchaudon, A., Modolo, R., Baskevitch, C.-A., Hess, L. G., Leclercq, L., Saur, J., Kimura, T., Kojima, H., Yagitani, S., and Miyoshi, Y.: The Radio & Plasma Wave Investigation (RPWI) for the JUpiter ICy moons Explorer (JUICE), Space Science Rev., 221, 1, https://doi.org/10.1007/s11214-024-01110-0, 2025.

Whipple, E. C., Warnock, J. M., and Winkler, R. H.: Effect of satellite potential on direct ion density measurements through the plasmapause, Journal of Geophysical Research: Space Physics, 79, 179–186, https://doi.org/10.1029/JA079i001p00179, 1974.

https://doi.org/10.5194/egusphere-2026-2030
Preprint. Discussion started: 22 April 2026


Yamauchi, M., Christon, S., Dandouras, I., Haaland, S., Kastinen, D., Kistler, L. M., Mann, I., Nozawa, S., Plane, J. M. C., Saito, Y., Schulz, L., Watababe, S., Wurz, P., and Yau, A. W.: Heavy Molecular and Metallic Ions in the Magnetosphere, Space Science Rev., 220, 82, https://doi.org/10.1007/s11214-024-01114-w, 2024.

Yue, C., Li, Y., Kistler, L., Ma, Q., Fu, H., Reeves, G. D., Zhou, X., Zong, Q., and Spence, H. E.: The Densities and Compositions of Background Cold Ions Based on the Van Allen Probe Observations, Geophysical Research Letters, 50, e2023GL104 282, https://doi.org/https://doi.org/10.1029/2023GL104282, e2023GL104282 2023GL104282, 2023.

Zeroual, M., Holmberg, M., Gutierrez, F., Johannsson, F., Wahlund, J.-E., Fraenz, M., Henri, P., Vallieres, X., and Fogg, A.: Surface charging of the JUICE spacecraft during the 2024 Earth gravity assist, Annales Geophysicae, 2026.